

From bare to renormalized order parameter in gauge space: Structure and reactions

G. Potel

National Superconducting Cyclotron Laboratory, Michigan State University, East Lansing, Michigan 48824, USA

A. Idini

Department of Physics, University of Surrey, Guildford, GU2 7HX, United Kingdom

F. Barranco

Departamento de Física Aplicada III, Escuela Superior de Ingenieros, Universidad de Sevilla, Camino de los Descubrimientos, E-41092 Sevilla, Spain

E. Vigezzi

INFN Sezione di Milano, Via Celoria 16, I-20133 Milano, Italy

R. A. Broglia

*Dipartimento di Fisica, Università degli Studi di Milano, Via Celoria 16, I-20133 Milano, Italy
and The Niels Bohr Institute, University of Copenhagen, DK-2100 Copenhagen, Denmark
(Received 31 May 2017; revised manuscript received 21 July 2017; published 12 September 2017)*

It is not physically obvious why one can calculate with similar accuracy, as compared to the experimental data, the absolute cross section associated with two-nucleon transfer processes between members of pairing rotational bands, making use of simple BCS (constant matrix elements) or of many-body [Nambu-Gorkov (NG), nuclear field theory (NFT)] spectroscopic amplitudes. Restoration of spontaneous symmetry breaking and associated emergent generalized rigidity in gauge space provides the answer and points to a new emergence: A physical sum rule resulting from the intertwining of structure and reaction processes, closely connected with the central role induced pairing interaction plays in structure, together with the fact that successive transfer dominates Cooper pair tunneling.

DOI: [10.1103/PhysRevC.96.034606](https://doi.org/10.1103/PhysRevC.96.034606)**I. INTRODUCTION**

The starting point of most descriptions of nuclear structure and reactions is based on independent particle motion. The validity of such a picture is related to basic quantum mechanics. Potential energy privileges fixed position between particles. On the other hand, fluctuations, in particular quantum fluctuations, favor symmetries. Regarding single-particle motion, such competition is embodied in the quantality parameter [1],

$$q = \frac{\hbar^2}{ma^2} \frac{1}{|v_0|}, \quad (1)$$

where m is the nucleon mass and v_0 and a are the strength and the range of the strong NN potential, respectively ($v_0 \approx -100$ MeV, $a \approx 1$ fm). The above equation is the ratio between the kinetic energy of confinement and the potential energy. Because $q \approx 0.4$, nucleons in the nucleus are delocalized, and mean field techniques can be used at profit in the description of nuclear structure.

II. SPONTANEOUS SYMMETRY BREAKING

The fact that basic properties of a quantal system can be described in terms of a mean field solution which does not display some of the symmetries of the original Hamiltonian, is known as the spontaneous symmetry-breaking phenomenon.

The lower symmetry mean field solution defines a privileged orientation in the corresponding three-dimensional (e.g., Nilsson) or gauge [e.g., BCS, Hartree-Fock-Bogoliubov (HFB)] space. All orientations have the same energy, in keeping with the fact that the restoring constant associated with changes in the Euler and gauge angles is zero. Fluctuations in orientation thus diverge in precisely the right manner to restore symmetry (see, e.g., Ref. [2], Secs. 4.2. and 4.2.3, and references therein). Because this divergence is associated with the vanishing of the frequency for constant inertia, the system acquires generalized rigidity (emergent property). Thus, acting with the specific external field (Cooper pair transfer in the case of pairing rotational band) sets the deformed system into rotation as a whole, without retardation effects. The above phenomena are at the basis of the broken symmetry restoration paradigm used to identify the elementary modes of nuclear excitation (see, e.g., Refs. [3] and references therein), in particular pairing rotations [3–8].

Pairing in nuclei has been introduced a number of times, first to explain the enhanced stability of even nuclei over odd nuclei [9], subsequently to describe the correlations associated with such staggering effects [10,11], after the BCS explanation of superconductivity [12,13] to account for the presence of a gap in the low-energy intrinsic excitation spectrum of deformed nuclei [14], and finally in connection with the advent of the Josephson effect, namely Cooper pair tunneling, and the

study of two-nucleon transfer processes, specific probes of deformation in gauge space [15,16].

A. Order parameter of nuclear superfluid phase

The order parameter associated with independent pair motion is defined as

$$\begin{aligned}\alpha'_0 &= \langle \text{BCS}(N+2) | P'^+ | \text{BCS}(N) \rangle, \\ &= \sum_j \sqrt{\frac{2j+1}{2}} B(j^2(0), N \rightarrow N+2),\end{aligned}\quad (2)$$

that is, the number of pairs participating in the BCS condensate. The quantity

$$\begin{aligned}B(j^2(0), N \rightarrow N+2) &= \langle \text{BCS}(N+2) | T'^+(j^2(0)) | \text{BCS}(N) \rangle \\ &= \sqrt{\frac{2j+1}{2}} U'_j(N) V'_j(N+2)\end{aligned}\quad (3)$$

is the two-nucleon transfer spectroscopic amplitude,

$$T'^+(j^2(0)) = \frac{[a_j'^+ a_j'^+]_0}{\sqrt{2}},\quad (4)$$

being the two-nucleon (Cooper pair) transfer operator, while

$$P'^+ = \sum_{jm>0} a'_{jm}{}^+ a'_{jm}{}^+ = \sum_j \sqrt{\frac{2j+1}{2}} T'^+(j^2(0))\quad (5)$$

is the operator which creates a pair of particles in time-reversal states. $|\text{BCS}(N)\rangle$ labels the BCS state for which the λ parameter (Fermi energy) has been adjusted so that $2 \sum_{jm>0} V_j'^2 = N$.

In keeping with (2), the order parameter $\alpha'_0 = \sum_j \left(\frac{2j+1}{2}\right) U'_j(N) V'_j(N+2) \approx \sum_j \left(\frac{2j+1}{2}\right) U'_j V'_j$ provides a measure of the nuclear deformation in gauge space and thus of the fact that the system displays a privileged orientation in this space, as can be seen from the relation (see Appendix A)

$$\begin{aligned}\alpha'_0 &= \sum_j \left(\frac{2j+1}{2}\right) U'_j V'_j \\ &= e^{2i\phi} \sum_j \left(\frac{2j+1}{2}\right) U_j V_j = e^{2i\phi} \alpha_0.\end{aligned}\quad (6)$$

The primed quantities are the BCS occupation amplitudes, which are referred to the intrinsic system of reference in gauge space (i.e., body-fixed BCS state), while the unprimed quantities are the same quantities referred to the laboratory system of reference. The two systems are connected by a rotation in gauge space of angle ϕ , induced by the operator $\mathcal{G} = \exp(-i\hat{N}\phi)$, where \hat{N} is the number operator and thus $a'_{jm}{}^+ = \mathcal{G}(\phi) a_{jm}^+ \mathcal{G}^{-1}(\phi)$ (see, e.g., Ref. [17] and references therein). It is notable that the phasing (A2) used in connection with Eq. (6) was chosen for somewhat historical reasons [18]. Using the more standard one, namely $U_\nu = U'_\nu e^{i\phi}$, $V_\nu = V'_\nu e^{-i\phi}$ (see Ref. [17] and references therein), the order parameter can be written as $\alpha_0 = \sum_{\nu>0} U_\nu^* V_\nu = e^{-2i\phi} \sum_{\nu>0} U'_\nu V'_\nu = e^{-2i\phi} \alpha'_0$.

A simple empirical confirmation that α_0 is the number of Cooper pairs of a superfluid nucleus can be made with

the help of the single j -shell model.¹ In this model, $V_j = (N/2\Omega)^{1/2}$ and $U_j = (1 - N/2\Omega)^{1/2}$, where $\Omega = (2j+1)/2$. For a system with $N = \Omega$ particles, i.e., $\Omega/2$ pairs, half-filled shell, typical of a superfluid nucleus, $V_j = U_j = (1/2)^{1/2}$ and $\alpha_0 = \Omega/2$. Thus, α_0 gives an estimate of the number of Cooper pairs which participate in specifying the orientation the $|\text{BCS}\rangle$ state has in gauge space. With the help of the approximate expression $\Omega = (2/3)A^{2/3}$, one obtains $\alpha_0 = 8$ for ^{120}Sn . Detailed microscopic calculations give values of $\alpha_0 = 5-6$ (see Sec. VI, Table II).

Symmetry restoration results from zero-point fluctuations of the gauge angle. They set the BCS deformed state into rotation, leading to pairing rotational bands, e.g., the ground state of superfluid Sn isotopes, where N plays in gauge space the role that angular momentum plays in quadrupole rotational motion. This symmetry restoration can be implemented by diagonalizing in the Quasi Random Phase Approximation (QRPA) the residual interaction H_{res} acting among quasiparticles that is neglected in the BCS mean field approximation (see Appendix A).

Since there are two parameters which determine the admixture of particle and hole states connected with gauge symmetry breaking, namely U_j and V_j (quasiparticle transformation), there are only two fields F which contribute to H_{res} through terms of the type FF^+ . One is antisymmetric with respect to the Fermi energy, namely $U_j^2 - V_j^2$, and leads to pairing vibrations of the gauge deformed state $|\text{BCS}\rangle$ (H'_p contribution to H_{res} , cf., e.g., Ref. [2], Appendix J). The other one, $U_j^2 + V_j^2$, is symmetric with respect to ϵ_F and leads to fluctuations which restore gauge symmetry (H''_p contribution to H_{res} , $H_{\text{BCS}} + H''_p$ commute with \hat{N}). Within this scenario, the field $U_j^2 - V_j^2$ excites two-quasiparticle states. By eliminating (in a particle-conserving fashion) this contribution from $U_j^2 + V_j^2$, one obtains the field that connects the members of ground-state rotational bands. That is, $[(U_j^2 + V_j^2)^2 - (U_j^2 - V_j^2)^2]^{1/2} \sim U_j V_j$. This result, together with (3) and (4), testifies to the fact that two-nucleon transfer reactions are, from the point of view of structure, the specific probes of pairing condensation in nuclei [19], as it emerges in a natural fashion by writing

$$\alpha_0 = \langle \text{BCS} | \sum_j \left(\sqrt{\frac{2j+1}{2}} T'^+(j^2(0)) \right) | \text{BCS} \rangle.\quad (7)$$

It is then natural that² the absolute two-nucleon-transfer cross section between members of a pairing rotational band

¹In the remainder of this paper, although we continue to refer all quantities to the intrinsic, body-fixed frame of reference in gauge space, we will not use primed letters, with the exceptions of particular cases which will be signaled and where the explicit appearance of the gauge angle ϕ is of use [cf., e.g., Appendix A, Eq. (A10)].

²Within this context, the Coulomb excitation cross section associated with the excitation of members of a quadrupole rotational band is proportional to Q_0^2 , the square of the quadrupole moment, a quantity which provides a measure of the number of aligned nucleons [3].

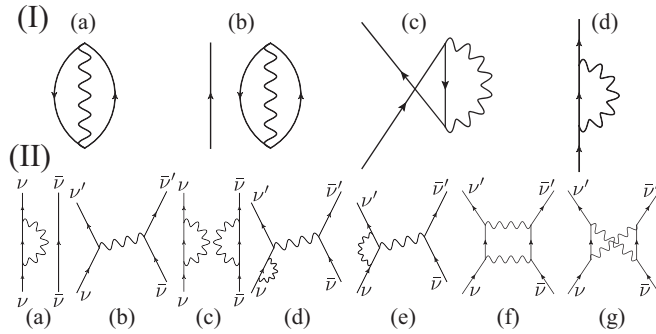


FIG. 1. (I) (a) ZPF associated with (particle-hole) surface vibrations, (b) odd system, (c) the antisymmetrization between the particles considered explicitly and those involved in the vibration; and (d) time ordering of panel (c). Diagrams (c) and (d) lead to the clothing of single-particle motion in lowest order in the particle-vibration coupling vertex. (II) A dressed nucleon moving in a state ν in the presence of (a) a bare nucleon moving in the time-reversed state $\bar{\nu}$ and (c) another dressed nucleon. Exchange of vibration in panel (a) leads to (b) the NFT lowest-order contribution in the particle-vibration coupling vertex of the induced pairing interaction (Appendix D). Exchange of vibrations in panel (c) leads to (d) self-energy, (e) vertex correction of the induced pairing interaction (Appendix E), and (f) ladder diagram contributing to the induced pairing interaction. The symmetrization between the bosons displayed in panel (c) is shown in panel (g).

can, schematically, be written as

$$\sigma \sim |\alpha_0|^2, \quad (8)$$

emphasizing again the close connection (unification) of structure and reaction aspects of the subject under discussion.

III. PHYSICAL NUCLEONS AND INDUCED PAIRING

In what follows, we will show that there is a simple physical reason at the basis of the above parlance, rooted in the fact that the atomic nucleus is a leptodermous finite many-body quantal system. Virtual states, like those associated with zero-point fluctuations (ZPF) of the nuclear vacuum (ground state), e.g., in which a surface quantised vibration and an uncorrelated particle-hole mode get virtually excited for a short period of time [Fig. 1(I)(a)], are a basic characteristic feature of these systems [20]. Adding a nucleon to it [odd system, Fig. 1(I)(b)] leads, through the particle-vibration coupling strength (V ; see, e.g., Ref. [21], Eq. (C6)) to processes which contain the effect of the antisymmetry between the single particle explicitly considered and the particles out of which the vibrations are built [Fig. 1(I)(c)]. Time ordering gives rise to the graph shown in Fig. 1(I)(d). Processes I(c) and I(d), known as correlation (CO) and polarization (PO) contributions to the mass operators (see Refs. [22,23], and references therein), clothe the particles, leading to physical nucleons whose properties can be compared with the experimental findings. Summing up, the processes shown in Fig. 1(I) are textbook examples of quantum field theory phenomena. They testify that the clothing of nucleons is at the basis of the quantal description of the atomic nucleus.

Nuclear superfluidity in general, and its incipience in the case of a single Cooper pair like in ^{11}Li in particular, are among the most quantal of all the phenomena displayed by the nuclear many-body system. Even if the 1S_0 , NN interaction was not operative, or was rendered subcritical by screening effects as in the case of ^{11}Li , Cooper binding will still be healthy, as a result of the exchange of vibrations between pairs of physical (clothed) nucleons moving in time-reversal states close to the Fermi energy [Figs. 1(II)(b), 1(II)(d)–1(II)(g)], a direct consequence of the ZPF of the nuclear vacuum (ground state) [Figs. 1(I)(a) and 1(I)(c)].³

Within this context, and only so, one can posit that the order parameter α_0 does not depend on the presence or absence of the 1S_0 , NN bare potential. Independent Cooper pair motion and thus nuclear superfluidity is intrinsically contained in the fluctuations of the quantal nuclear vacuum. As such, it is a truly emergent many-body nuclear property, implying generalized rigidity in gauge space, with the associated pairing rotational bands being specifically excited through pair transfer [3,4,6,7]. The fingerprint of spontaneous symmetry breaking

³Let us note that the Hamiltonian contains the Newtonian quantitative expression for causation in the potential energy, the classical idea of force. If, for instance, particles are acting on one another with a Coulomb force (as protons in the nucleus or the nucleus and the electrons in an atom), there appears in H the same timeless action over finite distance as in Newtonian mechanics. These vestiges of classical causality can give rise to serious problems under certain circumstances (cf., e.g., Refs. [24–26]), problems which are eliminated by taking into account the fact that the Coulomb interaction arises from the exchange of photons between charged particles. It is interesting to quote from the notes of Feynman on the self-interaction of two particles: “the self energy of two electrons is not the same as the self-energy of each one separately. That is because among the intermediate states which one needs in calculating the self-energy of particle number 1, say, the state of particle 2 can no longer appear in the sum because a transition of 1 into the state of 2 is excluded by the Pauli exclusion principle. The amount by which the self-energy of two particles differs from the self-energy of each one separately is actually the energy of their electric attraction” (see Ref. [27], p. 235). Fluctuations, in quantum mechanics, not only enter through the kinetic energy but also through the potential energy. Because of Heisenberg’s indeterminacy relations and Born-Jordan commutation laws, the quantal many-body system even in its ground state is at a finite, effective temperature, and the separation between enthalpies (potential) and entropic (kinetic) components is not clear cut, as forces are also ω -dependent many-body phenomena which only approximately can be treated in terms of static terms. In other words, the central issue in the quest of solving the many-body problem is that of having a correct description of the ground state as far as it reflects the virtual excitation of the system (Appendix B). This is the reason why effective field theories in general and NFT in particular have a good starting point, while *ab initio* calculations have to create it at each stage. While this task may not be too complicated to describe the effect of ZPF associated with giant resonances, that associated with low-lying collective modes is likely more trying. On the other hand, these states play the dominant role, through their state-dependent ZPF, in determining the texture of the nuclear physical vacuum and the nuclear properties at large.

in finite many-body systems is the presence of rotational bands associated with symmetry restoration. To qualify as a rotational band, a set of levels must display enhanced transition probabilities (absolute cross sections) associated with the operator having a nonvanishing value in the (degenerate) ground state (order parameter). In the present case (pairing rotational bands), this is the two-nucleon transfer operator [17,28]. In other words, cross talk (absolute transfer cross sections) between a member of a pairing rotational band and states not belonging to it should be much smaller than between members of the band. It could be argued that also important for the characterization of a pairing rotational band is the parabolic dependence of the energy with particle number. This is true, but many nonspecific effects can modify this dependence without altering the gauge kinship (common |BCS)-like intrinsic state). Before ascribing to two-nucleon transfer processes the role of specific probe not only from the point of view of nuclear structure but also from the vantage point of nuclear reactions,⁴ a central issue concerning the reaction mechanism should be clarified.

Considering that in superfluid nuclei lying along the stability valley, e.g., the Sn-isotopes, about half of the neutron pairing gap is associated with the induced pairing interaction [29,30], that is, $\Delta_{\text{ind}} \approx g_{pv}\alpha_0 = \Delta_{\text{exp}}/2 \approx 0.8$ MeV, where g_{pv} is the particle-vibration coupling parameter (equal to minus the induced pairing interaction). The mass enhancement factor λ [i.e., $m_\omega = m(1 + \lambda) \approx 1.4m$; see, e.g., Refs. [22] and [21], Eq. (C11)] can be written as $\lambda = g_{pv}N(0) (\approx 0.4)$, and therefore one obtains

$$N(0) \approx \frac{1}{2}\alpha_0 \text{ MeV}^{-1} \approx 4 \text{ MeV}^{-1} \quad (9)$$

for the density of neutron levels of, e.g., $^{120}\text{Sn}_{70}$ at the Fermi energy and for one spin orientation, as experimentally observed [$a \approx N/8 \text{ MeV}^{-1}$ for both spin orientations; see Ref. [31], Eq. (7.16)].

As a consequence of Eqs. (8) and (9),

$$\sigma \sim [N(0)]^2. \quad (10)$$

In other words, Cooper pair tunneling in nuclei is dominated by successive transfer. The significance of this result becomes clearer by recalling the fact that, according to Fermi's golden rule, processes like tunneling or decay are associated with a linear decay width in the density of states.

One can then argue that successive transfer may imply pair breaking, making two-nucleon transfer reactions a less-than-ideal probe of pairing correlations in nuclei. This is not true, however, a fact which can be understood by calculating the correlation length, that is, the range over which Cooper pair

partners, correlated by the exchange of collective vibrations, feel the presence of each other. One obtains⁵

$$\xi_{\text{ind}} = \frac{\hbar v_F}{\pi \Delta_{\text{ind}}} = \frac{\hbar v_F}{\pi g_{pv}\alpha_0} = \frac{\hbar v_F N(0)}{\pi \lambda \alpha_0} \approx 24 \text{ fm}. \quad (11)$$

In carrying out the above estimate, use has been made of $v_F/c = 0.3$, $\lambda = 0.4$, and $\alpha_0 = 8$. As a result, the generalized pair quantity parameter

$$q_{\xi_{\text{ind}}} = \frac{\hbar^2}{(2m)\xi_{\text{ind}}^2} \frac{1}{g_{pv}\alpha_0} \approx \frac{\hbar^2}{2m\xi_{\text{ind}}^2} \frac{N(0)}{\lambda\alpha_0} \approx 0.04 \quad (12)$$

has a value much smaller than 1, implying potential energy dominance and thus a strong correlation of the two partner nucleons of the Cooper pair over distances of the order of ξ , a quantity larger than nuclear dimensions. This result testifies to the fact that successive transfer of nucleons fully probes the nuclear pair correlations.

The wave functions of the nucleons in the pair are phase coherent, so one has to add the transfer amplitudes before taking the modulus square. The nucleons do not tunnel independently of each other but act more like a single particle, and the probability of a pair being transferred is comparable to the probability for the single-nucleon transfer process. It is like interference in optics with phase-coherent wave mixing. By denoting P_1 and P_2 as the single- and pair-nucleon transfer probability,⁶ one can write

$$P_2 = \left| \frac{1}{\sqrt{2}}(e^{i\phi'} U \sqrt{P_1} + e^{i\phi} V \sqrt{P_1}) \right|^2 \\ = P_1 \frac{(1 + 2UV \cos \epsilon)}{2} \approx P_1, \quad (\epsilon \equiv \phi - \phi'), \quad (13)$$

where the assumption was made that $\epsilon = 0$ and $U = V = 1/\sqrt{2}$, which makes use of the fact that the single-pair wave function is $(U_v + V_v e^{-i2\phi} a_v^+ a_v^+) |0\rangle$ and of the single- j shell estimate of the BCS occupation amplitudes.

In summary, in the reaction $^{120}\text{Sn} + p \rightarrow (^{119}\text{Sn} + d) \rightarrow ^{118}\text{Sn} + t$, the first neutron of the Cooper pair picked up by the proton to constitute the (virtual) deuteron can be at the surface of the nucleus close to the proton, while the second one can be at the antipode (diameter ≈ 12 fm). Eventually, the second one is transferred to form the triton within the interaction range (≈ 2 fm). This scenario involves relative distances between the partners of a Cooper pair, one in the target and the other one in the (virtual) deuteron, of the order of 10–14 fm [see Fig. 2, where the inner (n_1) orbital motion is to be interpreted to schematically describe clockwise motion and the external one (n_2) describes anticlockwise motion]. Thus, transfer of a rather extended object made out of two neutrons moving in time-reversal states is still correlated as a single-particle of

⁴Within this context, one may mention that while, e.g., (p,t) reactions are quite attractive processes to learn about pairing in nuclei, the s -relative motion of the two transfer nucleons is quite different in the target nucleus, e.g., ^{120}Sn , than in the outgoing triton (Ω_n overlaps, [28]). Inducing Cooper pair transfer with heavy ions allows one to better probe the s correlations. On the other hand, the simultaneous opening of many other channels makes the analysis of such reactions more involved and, arguably, less reliable.

⁵In keeping with the fact that $\Delta_{\text{ind}} \approx \Delta_{\text{exp}}/2$ as stated above, the actual Cooper pair mean square radius of ^{120}Sn , i.e., the order parameter, is about half the value (11).

⁶Single-particle $^{120}\text{Sn}(p,d)^{119}\text{Sn}$ and two-nucleon transfer $^{120}\text{Sn}(p,t)^{118}\text{Sn}$ (g.s.) absolute cross sections are in both cases of the order of a few mb (see Ref. [30] and references therein).

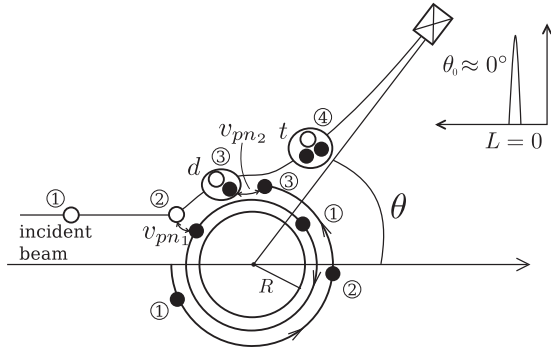


FIG. 2. Schematic representation of Cooper pair transfer in the reaction $^{120}\text{Sn}(p,t)^{118}\text{Sn}$ (g.s.) leading to essentially a single peak in the spectrum at 0° (after [19], Figs. 1(II)(b) and 1(II)(c) of this reference).

mass $2m^*$, in keeping with the estimated value of ξ and the phase coherence expressed by the relation $P_2 \approx P_1$.

Following standard practice, we refer throughout this paper to structure and reactions as two separate issues in the study of the atomic nucleus. While likely pedagogic, such an approach is fundamentally wrong, as already suggested in the abstract. In a nutshell, structure and reactions are two aspects of the same subject. One likely involves bound, the other continuum states, a distinction which is not even operative universally and certainly not in the case of light exotic halo nuclei. But even more important, because in quantum mechanics, nonmeasurable aspects of the system under study can hardly be called physical.

Within this context, the quantity (6) modulus squared can be measured only when each of its terms are properly weighted by the form factors (i.e., successive as well as simultaneous and nonorthogonal functions) and energy denominators (Green's functions), as forcefully expressed in (7) (see Appendix A, Eq. (A.21) of Ref. [19], and also Sec. III, Eq. (38(b)) of Ref. [17] as well as Figs. 2 and 12 of Ref. [32]). Consequently, when discussing the order parameter α_0 , in particular concerning the possible emergence of a physical sum rule, we are aware of

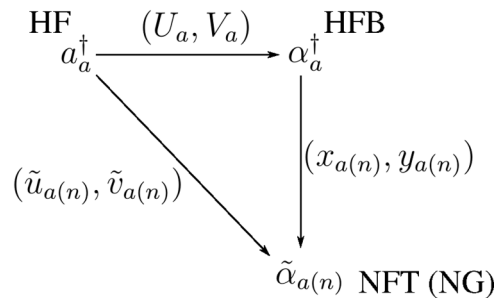


FIG. 3. Schematic representation of the generalized quasiparticle transformations from independent particle states $a_a^\dagger|0\rangle = |a\rangle$, to many-body clothed quasiparticle states $|a(\equiv(lj)(n))\rangle = \tilde{\alpha}_{a(n)}^+|\tilde{0}\rangle$, ($\tilde{\alpha}_{a(n)}^+ = \tilde{u}_{a(n)}a_a^\dagger - \tilde{v}_{a(n)}a_a$), made also in terms of a two-step protocol used in the present paper, implemented in terms of a quasiparticle transformation from Hartree-Fock (a_a^\dagger) to Hartree-Fock-Bogoliubov (α_a^\dagger) and a (self-energy based) rotation [see Eq. (20)].

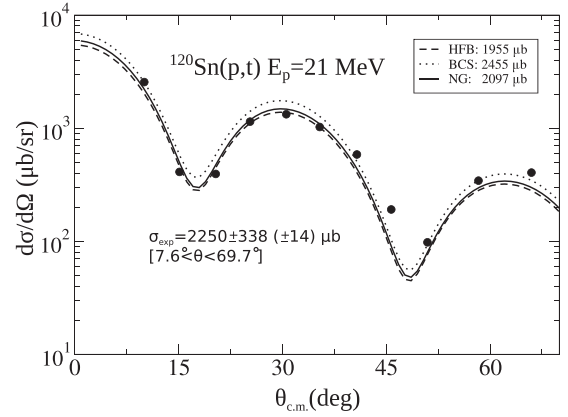


FIG. 4. Absolute differential cross sections associated with the reaction $^{120}\text{Sn}(p,t)^{118}\text{Sn}$ (g.s.) calculated making use of the BCS, HFB, and renormalized NFT(NG) spectroscopic amplitudes (Table II) and global optical parameters (Table III), in comparison with the experimental findings (solid dots) [43].

this fact even if, for simplicity, we do not state it explicitly. In other words, when talking about $|\alpha_0|^2$, the ultimate reference is to the results displayed in Figs. 4 and 5, namely predicted observables (absolute differential cross section) in comparison with the experimental findings. This implies that each term of α_0 has to be viewed as the weighted $j^2(0)$, mainly successive, form factor associated with independent pair motion, similar to the way in which talking about one-nucleon transfer, independent particle motion implies a spectroscopic amplitude and a radial form factor, also renormalized if that is the case (see, e.g., Ref. [33] and references therein). While the results contained in Tables I and II play an important role in the calculation of observables, the different entries still refer to the assessment of theory against theory.

With the above proviso, we can state that in keeping with the fact that $|\text{BCS}\rangle$ is a coherent state displaying off-diagonal

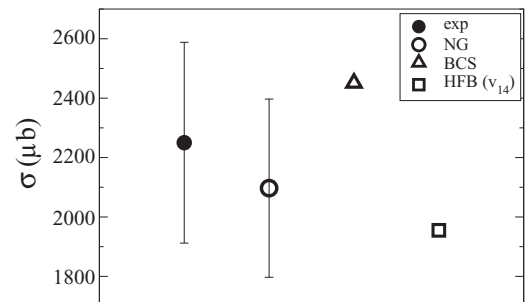


FIG. 5. Integrated absolute cross sections associated with the reaction $^{120}\text{Sn}(p,t)^{118}\text{Sn}$ (g.s.) (see caption to Fig. 4). The error ascribed to the NFT(NG) theoretical results stems from the uncertainties in the calculation of the corresponding two-neutron transfer spectroscopic amplitudes estimated from the variations the contribution of spin modes associated with different Skyrme interactions induce in the B coefficients.

TABLE I. In the first four columns, we list the orbital, its HF energy ϵ_a calculated with the SLy4 interaction, and the renormalized energy $\tilde{\epsilon}_{a(n)}$ of the main n peaks resulting from the breaking of the strength due to renormalization effects, with the numeral n being given in the fourth column. In the next six columns, we list the renormalized quasiparticle energies, occupation factors, total quasiparticle strength, Z factor, and state-dependent gap of the lowest peaks associated with each of the five valence levels in ^{120}Sn , carrying more than 5% of the single-particle strength. In the other columns, we list quasiparticle energies and occupation factors obtained in a HFB calculation with the Argonne interaction (v_{14}) ($\Delta^{\text{HFB}} = 1.08$ MeV) and with a monopole force of strength $G = 0.26$ MeV, fitted to reproduce the empirical three-point value $\Delta^{\text{exp}} \approx 1.45$ MeV. This last calculation is equivalent to BCS. In all cases, the energy of the $d_{5/2}$ level has been shifted by 600 keV toward the Fermi energy [30]. In the renormalized calculation, spin modes have been effectively taken into account by including a repulsive monopole interaction of strength $G = 0.03$ MeV acting on the valence orbitals in the solution of the Nambu-Gorkov equation (quantitative effect of spin modes).

a	ϵ_a	$\tilde{\epsilon}_{a(n)}$	n	$\tilde{E}_{a(n)}$	$\tilde{u}_{a(n)}^2$	$\tilde{v}_{a(n)}^2$	$N_{a(n)}$	$Z_{a(n)}$	$\tilde{\Delta}_{a(n)}$	$E_a(v_{14})$	$U_a^2(v_{14})$	$V_a^2(v_{14})$	$E_a(G)$	$U_a^2(G)$	$V_a^2(G)$
$d_{5/2}$	-10.7	-9.4	1	2.55	0.06	0.28	0.34	0.60	1.96	3.12	0.03	0.97	3.09	0.06	0.94
		-9.9	2	2.75	0.01	0.10	0.11		1.80						
		-10.5	3	3.19	0.01	0.10	0.11		1.68						
		-10.6	4	3.36	0.01	0.07	0.08		1.88						
		-11.2	5	3.95	0.01	0.07	0.08		1.97						
		-12.4	6	4.77	0.0	0.07	0.07		-1.29						
		-12.7	7	4.98	0.0	0.09	0.09		-0.61						
$g_{7/2}$	-10.1	-9.3	1	2.10	0.09	0.59	0.68	0.78	1.43	2.56	0.06	0.94	2.54	0.09	0.91
		-10.6	2	2.83	0.00	0.08	0.08		0.34						
		-9.9	3	3.20	0.00	0.0	0.0		-2.40						
		-11.2	4	3.50	0.00	0.11	0.11		0.97						
$s_{1/2}$	-9.0	-8.4	1	1.80	0.26	0.53	0.79	0.72	1.69	1.61	0.13	0.87	1.79	0.22	0.78
		-10.4	2	2.84	0.00	0.04	0.04		-1.03						
		-10.1	3	3.20	0.00	0.0	0.0		-2.20						
		-12.4	4	4.64	0.00	0.07	0.07		-0.46						
$d_{3/2}$	-8.5	-7.9	1	1.48	0.38	0.46	0.84	0.76	1.48	1.37	0.24	0.76	1.57	0.33	0.67
		-7.5	2	2.75	0.0	0.00	0.0		-2.73						
		-8.8	3	3.06	0.0	0.01	0.01		-2.88						
		-11.3	4	3.49	0.0	0.05	0.05		-0.14						
$h_{11/2}$	-7.1	-7.2	1	1.64	0.57	0.26	0.83	0.79	1.52	1.34	0.79	0.21	1.74	0.77	0.23
		-4.7	2	3.08	0.09	0.00	0.09		0.08						
		-9.6	3	3.97	0.00	0.00	0.0		3.54						

long-range order⁷ (ODLRO; see Appendix A), one expects (8) to be a physically conserved quantity. Also, the robustness of the order parameter α_0 to characterize nuclear superfluidity as compared to the pairing gap is testified by the fact that α_0 is different from zero also in nuclear regions, like between two heavy ions at the distance of closest approach in, e.g.,

the process $a(=b+2)+A \rightarrow b+B(=A+2)$, a situation in which the pairing interaction and thus also Δ are zero.⁸

Let us conclude this section by noting that while the expression (13) displays, in a simple way, the gauge phase coherence associated with independent pair motion, it does not contain the independent particle limit, lacking the energy denominator. Of course, this limit is simple to exhibit in the quantal [17] or semiclassical [19] formalism mentioned above, which has the drawback of becoming involved in connection with phase gauge coherence.

IV. MANY-BODY ASPECTS OF THE NUCLEAR PAIRING INTERACTION

While in condensed matter the many-body aspects of the pairing interaction could not be ignored, this could happen in nuclear physics. This is primarily because the electron-

⁷Within this context, note that the overall gauge phase ensuring that |BCS) is a coherent state in this space, is the same as the one at the basis of the Josephson effect. In fact, the Josephson effect provided the first (only) specific probe to measure the gauge angle (difference) in superconductors. Now, because in condensed matter there are a number of phenomena like supercurrents, Meissner effect, etc., which testify to pair condensation, the direct relation existing between ODLRO and the Josephson effect has not been at center stage. However, the situation is completely different in the case of atomic nuclei, where supercurrents cannot be observed, in keeping with the fact that $\xi \gg R_0$. Consequently, Cooper pair transfer is essential to probe nuclear superfluidity and associated gauge space coherence.

⁸Using an analogy, the deformation of a 3D-quadrupole-rotating system is measured by the quadrupole moment Q_0 , and not by the field approximation (κQ_0) to the separable quadrupole-quadrupole interaction $H_Q = -\kappa(QQ)$.

TABLE II. Two-nucleon spectroscopic amplitudes [Eqs. (3) and (33)] and contributions to α_0 [$(j_a + 1/2)^{1/2} B(a)$] calculated making use of the quantities given in Table I. In the last row, the value of α_0 is reported while the percentage of the number of neutrons (i.e., $2\alpha_0/70$) participating in the condensate is given in parentheses. In the last column, the quantities worked out making use of the approximation (34) for $\tilde{u}_{a(n)}$ and $\tilde{v}_{a(n)}$ are given.

$a \equiv \{l_j\}$	$B(a) [(\alpha_0)_a]$			
	NFT(NG)	HFB(v_{14})	BCS(G)	Z BCS(G)
$d_{5/2}$	0.43 (0.74)	0.29 (0.51)	0.41 (0.71)	0.40(0.70)
$g_{7/2}$	0.46 (0.92)	0.47 (0.95)	0.57 (1.14)	0.45(0.89)
$s_{1/2}$	0.37 (0.37)	0.34 (0.34)	0.41 (0.41)	0.30(0.30)
$d_{3/2}$	0.59 (0.84)	0.60 (0.85)	0.66 (0.94)	0.50 (0.71)
$h_{11/2}$	0.95 (2.34)	1.0 (2.44)	1.03 (2.52)	0.81(1.99)
α_0	5.21 (15%)	5.09(15%)	5.74(16%)	4.59(13%)

electron bare interaction is repulsive (Coulomb), but also because the highest values of T_c in low-temperature metallic superconductors are, as a rule, associated with bad conductors at room temperature, underscoring the role played by the electron-phonon coupling in the superconducting phenomenon and the need for a correct treatment of this interaction. In other words, the scenario of the Nambu-Gorkov and Eliashberg approach to superconductivity [34–36].

In nuclear physics, on the other hand, the values of 1S_0 phase shifts are positive for low values of the relative nucleon velocities ($E_{\text{lab}} \leq 200$ MeV), and the particle-vibration coupling mechanism is still often thought to give only rise to self-energy phenomena. As a result, it was assumed that the nuclear pairing interaction was short range and resulted solely from meson exchange, with long-range interactions being responsible for mean field effects (see, e.g., Ref. [37] for a review of this nuclear model, and references therein). This attitude has proven to be difficult to overcome. In other words, like the fact that one cannot measure the bare nucleon mass in nuclei but the clothed one [see Figs. 1(I)(c) and 1(I)(d)], one cannot measure the bare pairing interaction in the nuclear medium but only the effective one, which is the sum of the bare (v_{bare}^p) and induced (v_p^{ind}) ones [see Figs. 1(II)(b), 1(II)(d)–1(II)(g)]. Furthermore, in nuclear physics as in condensed matter, a nonperturbative treatment of the particle-vibration coupling (PVC) is needed in a number of cases, e.g., in connection with the breaking of the $d_{5/2}$ orbit of ^{120}Sn . Within the framework of Nuclear Field Theory (NFT), by applying the Nambu-Gorkov (NG) technique developed to describe metallic superconductors to this open shell nucleus, it is possible to obtain a complete characterization of it. The theoretical predictions reproduce the experimental results to within the 10% level [30]. As we shall see below, the contributions of the many-body effects related to the one-particle channel do not affect the absolute two-nucleon transfer reaction cross section in any major way. This fact testifies to the robustness of α_0 , in the sense of two-nucleon transfer spectroscopic amplitude as explained in Sec. III, and to the physical soundness of making it the nuclear superfluid order parameter.

V. ELEMENTARY MODES OF EXCITATION: EMPIRICAL RENORMALIZATION IN STRUCTURE AND REACTIONS

The elementary modes of excitation of a many-body system represent a generalization of the idea of normal modes of vibration. They constitute the building blocks of the excitation spectra, providing insight into the deep nature of the system one is studying, aside from allowing for an economic description of complicated spectra in terms of a gas of, as a rule, weakly interacting bosons and fermions. In the nuclear case, they correspond to clothed particles and empirically renormalized vibrations (rotations).

Two ideas lie behind the concept of elementary modes of excitation: first, that one does not need to be able to calculate the total binding energy of a nucleus to accurately describe the low-energy excitation spectrum, in much the same way in which one can calculate the normal modes of a metal rod not knowing how to calculate its total cohesive energy. The second idea is that low-lying states ($\hbar\omega \ll \epsilon_F \ll BE$) are of a particularly simple character and are amenable to a simple treatment. Their interweaving is carried out at profit, in most cases, in perturbation theory.⁹ Within this context, it is necessary to have a microscopic description of the ground state of the system which ensures that it acts as the vacuum state $|\tilde{0}\rangle$ of the elementary modes of excitation. In other words, $a_\nu|\tilde{0}\rangle = 0, \Gamma_\alpha|\tilde{0}\rangle = 0$, where $a_\nu^+|\tilde{0}\rangle = |\nu\rangle$ and $\Gamma_\alpha^+|\tilde{0}\rangle = |\alpha\rangle$ represent a single particle and a one-phonon state, respectively. This implies, in keeping with the indeterminacy relations $\Delta x \Delta p \geq \hbar/2$, that $|\tilde{0}\rangle = |0\rangle_F |0\rangle_B$ displays quantal zero-point fluctuations (ZPF).

Within the framework of nuclear field theory (NFT) used below, in which single-particle (fermionic, F) and vibrational (bosonic, B) elementary modes of excitation are to be calculated within the framework of HFB and QRPA respectively, $|\tilde{0}\rangle$ must display the associated ZPF (cf. Appendix B). In particular, for (harmonic) vibrational modes $\Delta x \Delta p = \hbar/2$, the associated zero-point energy amounts to $\hbar\omega/2$ for each degree of freedom, e.g., $5\hbar\omega/2$ for quadrupole vibrations, with $\hbar\omega$ being the energy of the collective vibrational mode under consideration.

An illustrative example of the above arguments is provided by the low-lying quadrupole vibrational state of ^{120}Sn . Diagonalizing SLy4 in QRPA leads to a value of $B(E2)$ ($890 e^2 \text{fm}^2$), which is about a factor of 2 smaller than experimentally observed ($2030 e^2 \text{fm}^2$). Taking into account renormalization effects in NFT, namely in a conserving approximation (self-energy and vertex corrections, generalized Ward identities),

⁹More precisely, and in keeping with the fact that boson degrees of freedom have to decay through linear particle-vibration coupling vertices into their fermionic components to interact with another vibrational mode, the interweaving between the variety of many-body components clothing a single-particle state or a collective vibration will be described at profit in terms of an arrowed matrix which, assuming perturbation theory to be valid, can be transformed, neglecting contributions of the order of g_{pv}^3 or higher, into a codiagonal matrix, namely a matrix whose nonzero elements are $(i, i-1)$ and $(i, i+1)$, aside from the diagonal ones (i, i) .

one obtains a value ($2150 \text{ e}^2 \text{ fm}^2$) which essentially coincides with the experimental findings. One does not know how to accurately calculate the absolute ground-state energy E_0 (total binding energy) of, e.g., ^{120}Sn , but one can do pretty well to work out the properties of the low-energy mode of this nucleus, the collective energies $\hbar\omega_L = E_L - E_0$, and thus the associated ZPF and zero-point energy E_0 by renormalizing QRPA solutions to lowest order through self-energy and vertex corrections contributions [29]. Now, if the collective phonons are not the main object of the study but are to be used to clothe the single-particle states and give rise to the induced pairing interaction, one can make use of phonons which account for the experimental findings (NFT renormalization [30]; see also Refs. [32,33]).

It is to be noted that in calculating the $E\lambda$ lifetimes, e.g., the quadrupole lifetime associated with the low-lying quadrupole mode [$T(E2) = 1.22 \times 10^9 \times E_\gamma^5 \times B(E2)$, $E_\gamma = \hbar\omega_{2+}$], the kinematic (E_γ^5) and structural [$B(E2)$] contributions can be treated separately. This is in keeping with the fact that in the case of electromagnetic decay as well as of anelastic processes, the relative motion coordinate is always that of the entrance channel, at variance with particle-transfer processes. Consequently, in connection with these processes, structure and reactions are treated separately, a possibility not operative in the case of transfer reactions. Let us extend this discussion to the particle-transfer process, in particular, to the two-particle pickup reaction $^{120}\text{Sn}(p,t)^{118}\text{Sn}(\text{g.s.})$. In this case, and to be able to calculate the radial dependence of successive transfer, everything has to be translated in terms of single-particle motion and associated absolute separation energies and radial wave functions in systems with different coordinates of relative motion.

If the k -mass connected with the Perey-Buck energy-dependent term [22] already made the concept of a single mean field potential somewhat illusory (Appendix C), consider the difficulties one is confronted with in attempting to translate into a description of single-particle motion inside a common potential, independent motion of Cooper pairs, composite bosonic particles with binding energies of the order of one tenth of the Fermi energy¹⁰ ($\approx 2\Delta/\epsilon_F \approx 3 \text{ MeV}/36 \text{ MeV}$) and a correlation length of tens of fm, subject to a strong external field of radius $R_0 \approx 6 \text{ fm}$ and depth $\approx 50 \text{ MeV}$. A way out of this situation is provided by the fact that in superfluid nuclei, one is not very far from an independent-particle picture. As a consequence, no major errors are introduced in treating the system accordingly, which is also in keeping with the fact that transfer takes place through the single-particle field [17].

In summary, while one does not know how to calculate the mass of the nucleus, one can accurately calculate $U_j(118)V_j(120)$, as well as the relative value of the clothed single-particle energies. In keeping with the fact that renormalized NFT, which makes use of the NG equation, correctly reproduces the quasiparticle energies, the Fermi energy of

the single-particle potential used to generate the radial wave function is adjusted so that the least bound state has the experimental separation energy S_n . Within the unified picture of structure and reactions (NFT ($r+s$), [32]), dressing the radial wave functions give rise to the correct form factors for transfer processes. While these effects are small for ^{120}Sn , they are overwhelming in other situations, e.g., that of halo nuclei [33].

VI. COOPER PAIR POPULATION OF PAIRING ROTATIONAL BANDS: BCS, HFB, AND NG

In what follows, we analyze the stability of the order parameter as probed by Cooper pair transfer.

A. BCS

Starting from a HF calculation with the SLy4 interaction (Table I, second column), we solve the BCS equations for ^{120}Sn and thus determine the corresponding occupation numbers $U_a(G)$ and $V_a(G)$ (Table I, last two columns) with a schematic monopole pairing force of strength $G = 0.26 \text{ MeV}$, adjusted to fit the empirical three-point value $\Delta^{\text{exp}} \approx 1.4 \text{ MeV}$.

B. HFB

Making use of the same Skyrme interaction and of the v_{14} Argonne, 1S_0 , NN potential and neglecting the influence of the bare pairing force in the mean field, we solved the HFB equation. As a result, this step corresponds to an extended BCS calculation over the HF basis, allowing for the interference between states of equal quantum numbers $a(\equiv lj)$, but different number of nodes (k, k'). To properly take into account the repulsive core of v_{14} in the calculation of Δ^{HFB} , we include for each a states up to $\approx 1 \text{ GeV}$. As a consequence, one obtains a set of quasiparticle energies E_a^μ , with the quasiparticle index ($\mu = 1, 2, \dots, N_a$). Each quasiparticle $\alpha_{a,\mu}^+ = \sum_{k=1}^{N_a} (U_a^{\mu,k} a_{a,k}^+ - V_a^{\mu,k} a_{a,k})$ is associated to an array of quasiparticle amplitudes $U_a^{\mu,k}$ and $V_a^{\mu,k}$, which are the components of the quasiparticles over the HF basis states $\phi_k^a = \langle \vec{r} | a_{a,k}^+ | 0 \rangle (\equiv \langle \vec{r} | a, k \rangle)$. Going to the canonical basis, where the density matrix takes a diagonal form, we look for the state having the largest value of the abnormal density, $(UV)_{\text{max}}$. As a rule, for a well-bound nucleus such as ^{120}Sn , this canonical state is the quasiparticle state having the lowest value of the quasiparticle energy. The label k then drops because there is only one orbital for a given value of $a(\equiv lj)$. This implies that the bare quasiparticle amplitudes can be characterized simply by U_a, V_a and the associated state-dependent value of the bare pairing gap is equal to $\Delta_a^{\text{bare}} = 2U_a V_a E_a$. The values of $(E_a)_{\text{min}}$ and $[V_a(v_{14})]_{\text{max}}$ for the five valence orbitals are reported in Table I.

C. Renormalized NFT and NG

We now go beyond mean field and include the particle-vibration coupling leading to retardation phenomena both in self-energy as well as in induced interaction processes. The vibrational modes are calculated in QRPA, making use of empirical Woods-Saxon (WS) single-particle levels, BCS with constant G , and multipole-multipole separable interactions of

¹⁰Within this context, we note that in ^{120}Sn the two-neutron separation energy is $S_{2n} = 15.6 \text{ MeV}$, while $S_{1n} = 9.1 \text{ MeV}$, i.e., $(2 \times S_{1n}) - S_{2n} = 2.6 \text{ MeV}$.

essentially self-consistent strength [3] which reproduce the observed properties of the low-lying collective states.

To be able to treat the variety of possible situations, we return to the full HFB basis. In this basis, the ω -dependent self-energy has the following matrix structure [38]:

$$\hat{\Sigma}_{\mu,\mu'}^a(\omega) = \begin{pmatrix} \Sigma_{\mu,\mu'}^{11,a}(\omega) & \Sigma_{\mu,\mu'}^{12,a}(\omega) \\ \Sigma_{\mu,\mu'}^{21,a}(\omega) & \Sigma_{\mu,\mu'}^{22,a}(\omega) \end{pmatrix}. \quad (14)$$

The Dyson equation,

$$\hat{G}^a(\omega + i\eta) = [\omega + i\eta - \hat{H}_{\text{HFB}} - \hat{\Sigma}^a(\omega + i\eta)]^{-1}, \quad (15)$$

provides the connection to the corresponding Green's function matrix. The imaginary part of this function is related to the strength functions that define energies and weights of the dressed quasiparticles,

$$\tilde{S}_{k,k'}^{a,+}(\omega) = -\frac{\text{Im}}{\pi} \left\{ \sum_{\mu,\mu'} G_{\mu,\mu'}^{11,a} U_a^{\mu,k} U_a^{\mu',k'} - G_{\mu,\mu'}^{12,a} U_a^{\mu,k} V_a^{\mu',k'} - G_{\mu,\mu'}^{21,a} V_a^{\mu,k} U_a^{\mu',k'} + G_{\mu,\mu'}^{22,a} V_a^{\mu,k} V_a^{\mu',k'} \right\}, \quad (16)$$

$$\tilde{S}_{k,k'}^{a,-}(\omega) = -\frac{\text{Im}}{\pi} \left\{ \sum_{\mu,\mu'} G_{\mu,\mu'}^{11,a} V_a^{\mu,k} V_a^{\mu',k'} + G_{\mu,\mu'}^{12,a} V_a^{\mu,k} U_a^{\mu',k'} + G_{\mu,\mu'}^{21,a} U_a^{\mu,k} V_a^{\mu',k'} + G_{\mu,\mu'}^{22,a} U_a^{\mu,k} U_a^{\mu',k'} \right\}, \quad (17)$$

$$\tilde{S}_{k,k'}^a(\omega) = -\frac{\text{Im}}{\pi} \left\{ \sum_{\mu,\mu'} G_{\mu,\mu'}^{11,a} U_a^{\mu,k} V_a^{\mu',k'} + G_{\mu,\mu'}^{12,a} U_a^{\mu,k} U_a^{\mu',k'} - G_{\mu,\mu'}^{21,a} V_a^{\mu,k} V_a^{\mu',k'} - G_{\mu,\mu'}^{22,a} V_a^{\mu,k} U_a^{\mu',k'} \right\}, \quad (18)$$

where $\tilde{S}_{k,k'}^{a,+}(\omega)$, $\tilde{S}_{k,k'}^{a,-}(\omega)$, and $\tilde{S}_{k,k'}^a(\omega)$ play the role of the probability density of the dressed quasiparticle, quasihole, and the corresponding anomalous component. It is also possible to express $\hat{\Sigma}$ as a function of \tilde{S}^+ , \tilde{S}^- , and \tilde{S} [38]. Thus one can carry out an iterative, self-consistent procedure to calculate quasiparticle renormalization, accounting for the so-called rainbow series. This formalism does not assume the validity of the quasiparticle approximation and iterates the solutions of the Dyson equations on the ansatz of continuous strength functions. However, close to the Fermi energy, quasiparticle peaks in the strength functions are clearly identifiable due to their characteristic Lorentzian shape, as implied by the extension to the complex plane introduced in (15) in terms of the parameter η [39]. Fitting these peaks, one can determine the centroid energy $\tilde{E}_{a(n)}$ (dressed quantities labeled with a tilde carry a sum over μ values [see Eqs. (16)–(18)]) and associated width $\tilde{\Gamma}_{a(n)}$ for the fragment n , as well as its occupation amplitudes $\tilde{u}_{a(n)}^k$ and $\tilde{v}_{a(n)}^k$.

Alternatively, one can obtain the same result, still with an accuracy fixed by the η parameter, but this time in terms of individual levels solving (at the last iteration) the eigenvalue Nambu-Gorkov equation,

$$[\hat{H}_{\text{HFB}} + \hat{\Sigma}^a(\tilde{E}_{a(n)})]_{k,k'} \begin{pmatrix} x_{a(n)}^{k'} \\ y_{a(n)}^{k'} \end{pmatrix} = \tilde{E}_{a(n)} \begin{pmatrix} x_{a(n)}^k \\ y_{a(n)}^k \end{pmatrix}. \quad (19)$$

The above formalism provides a most general framework to deal with the nuclear many-body problem, also in situations in which repulsive core and ω -dependent soft-mode-mediated interactions are active (see, e.g., Ref. [40]). In the case of well-bound nuclei lying along the stability valley, as in the present case, the above equations can be simplified by turning to the canonical basis and, in keeping with the fact that the particle-vibration couplings are mostly effective in a small region around the Fermi energy, it is possible to restrict the phase space of the calculations to the valence orbitals.

Within this scenario, we introduce the shorthand notation $\Sigma_{a(n)}^{ij} \equiv \Sigma^{ij,a}(\tilde{E}_{a(n)})$ for $i, j = 1, 2$. It is convenient to define the renormalized quasiparticle amplitudes associated with a given solution $a(n)$ as

$$\begin{aligned} \tilde{u}_{a(n)} &= x_{a(n)} U_a - y_{a(n)} V_a, \\ \tilde{v}_{a(n)} &= x_{a(n)} V_a + y_{a(n)} U_a. \end{aligned} \quad (20)$$

The above quantities are the quasiparticle amplitudes of the renormalized state $|\tilde{a}(n)\rangle$. The total quasiparticle strength associated with the n th fragment is (see Fig. 3)

$$\tilde{N}_{a(n)} = \tilde{u}_{a(n)}^2 + \tilde{v}_{a(n)}^2. \quad (21)$$

The matrix elements of the total self-energy, rotated into the canonical basis and identified in terms of primed quantities including the bare interaction and the particle-phonon coupling, are given by

$$\begin{aligned} \tilde{\Sigma}_{a(n)}^{11'} &= U_a^2 \tilde{\Sigma}_{a(n)}^{11} + V_a^2 \tilde{\Sigma}_{a(n)}^{22} - 2U_a V_a \tilde{\Sigma}_{a(n)}^{12}, \\ \tilde{\Sigma}_{a(n)}^{22'} &= U_a^2 \tilde{\Sigma}_{a(n)}^{22} + V_a^2 \tilde{\Sigma}_{a(n)}^{11} + 2U_a V_a \tilde{\Sigma}_{a(n)}^{12}, \\ \tilde{\Sigma}_{a(n)}^{12'} &= \Delta_a^{\text{bare}} + (\tilde{\Sigma}_{a(n)}^{12})'_{\text{ind}}, \end{aligned} \quad (22)$$

$$(\tilde{\Sigma}_{a(n)}^{12})'_{\text{ind}} \equiv \tilde{\Sigma}_{a(n)}^{12} (U_a^2 - V_a^2) + U_a V_a (\tilde{\Sigma}_{a(n)}^{11} - \tilde{\Sigma}_{a(n)}^{22}). \quad (23)$$

The total pairing gap is equal to

$$\tilde{\Delta}_{a(n)} = \tilde{Z}_{a(n)} (\tilde{\Sigma}_{a(n)}^{12})', \quad (24)$$

with the Z factor [41] being

$$\tilde{Z}_{a(n)} = \left(1 - \frac{\tilde{\Sigma}_{a(n)}^{\text{odd}}}{\tilde{E}_{a(n)}} \right)^{-1}, \quad (25)$$

where

$$\tilde{\Sigma}_{a(n)}^{\text{odd}} = \frac{\tilde{\Sigma}_{a(n)}^{11} + \tilde{\Sigma}_{a(n)}^{22}}{2}. \quad (26)$$

It is of notice that for levels close to the Fermi energy $\tilde{\Sigma}_{a(n)}^{\text{odd}}/\tilde{E}_{a(n)}$ approaches a derivative, and the physical role of $\tilde{Z}_{a(n)}$ approaches that of $\tilde{N}_{a(n)}$, namely the quasiparticle component in the many-body renormalized quasiparticle state $|\tilde{a}(n)\rangle$.

We can identify two contributions to the pairing gap $\tilde{\Delta}_{a(n)}$:

$$\tilde{\Delta}_{a(n)} = [\tilde{Z}_{a(n)} \Delta_a^{\text{bare}}] + [\tilde{Z}_{a(n)} (\tilde{\Sigma}_{a(n)}^{12})'_{\text{ind}}]. \quad (27)$$

The first one is related to the pairing gap associated with the bare force and quenched by the many-body effects which

TABLE III. Optical potentials used in the calculation of the absolute two-nucleon transfer differential cross sections. The quantities V , W , V_{so} , W_d are in MeV while the remaining quantities are in fm. The nuclear term of the optical potential was chosen to have the form $U(r) = -Vf_1(r) - iWf_2(r) - 4iW_d g_3(r) - (\frac{\hbar}{m_\pi c})^2 V_{so} \frac{g_4(r)}{a_4 r} \mathbf{1} \cdot \mathbf{s}$, with $f_i(r) = \frac{1}{1+e^{(r-R_i)/a_i}}$; $g_i(r) = \frac{e^{(r-R_i)/a_i}}{(1+e^{(r-R_i)/a_i})^2}$, and m_π being the pion mass, while $R_i = r_i A^{1/3}$, with A being the mass number of the heavy nucleus in the corresponding channel. The Coulomb term is taken to be the electrostatic potential generated by an uniformly charged sphere of radius R_1 .

	${}^A\text{Sn}(p,t){}^{A-2}\text{Sn}$											
	V	W	V_{so}	W_d	r_1	a_1	r_2	a_2	r_3	a_3	r_4	a_4
$p, {}^A\text{Sn}^a$	50	5	3	6	1.35	0.65	1.2	0.5	1.25	0.7	1.3	0.6
$d, {}^{A-1}\text{Sn}^b$	78.53	12	3.62	10.5	1.1	0.6	1.3	0.5	0.97	0.9	1.3	0.61
$t, {}^{A-2}\text{Sn}^a$	176	20	8	8	1.14	0.6	1.3	0.5	1.1	0.8	1.3	0.6

^aReference [43].

^bReference [59].

clothe the bare nucleons. The second contribution obeys a generalized gap equation [42],

$$(\tilde{\Sigma}_{a(n)}^{12})'_{\text{ind}} = - \sum_{b,m} \frac{(2j_b + 1)}{2} \times \langle b(m)\overline{b(m)} | v_{\text{ind}} | a(n)\overline{a(n)} \rangle \tilde{u}_{b(m)} \tilde{v}_{b(m)}, \quad (28)$$

where the induced interaction v_{ind} is associated with the exchange of collective vibrations between pairs of nucleons moving in time reversal states. The matrix element in Eq. (28) is (see Appendix D)

$$\begin{aligned} & \langle b(m)\overline{b(m)} | v_{\text{ind}} | a(n)\overline{a(n)} \rangle \\ &= \sum_{\lambda,\nu} \frac{2|h(a,b\lambda\nu)|^2}{(2j_b + 1)} \left[\frac{1}{\tilde{E}_{a(n)} - \tilde{E}_{b(m)} - \hbar\omega_{\lambda\nu}} \right. \\ & \quad \left. - \frac{1}{\tilde{E}_{a(n)} + \tilde{E}_{b(m)} + \hbar\omega_{\lambda\nu}} \right], \quad (29) \end{aligned}$$

where $h(a,b\lambda\nu)$ denotes the matrix element coupling the particle a to the configuration $(b \otimes \lambda\nu)_a$, while the energy of the ν th phonon of multipolarity λ is denoted $\hbar\omega_{\lambda\nu}$ [3]. Concerning vertex correction to both v_{ind} and v_{bare} , we refer readers to Appendix E.

The selection of the basis $|\tilde{a}(n)\rangle = \tilde{\alpha}_{a(n)}^+ |\tilde{0}\rangle$ through the rotation (20) allows the eigenvalues of (19) to retain the standard BCS relation, namely,

$$\tilde{E}_{a(n)} = \sqrt{(\tilde{\epsilon}_{a(n)} - \epsilon_F)^2 + (\tilde{\Delta}_{a(n)})^2}, \quad (30)$$

with the renormalized quasiparticle energy being

$$\tilde{\epsilon}_{a(n)} - \epsilon_F = \tilde{Z}_{a(n)} [(\epsilon_a - \epsilon_F) + \tilde{\Sigma}_{a(n)}^{\text{even}'}], \quad (31)$$

where

$$\tilde{\Sigma}_{a(n)}^{\text{even}'} = \frac{\tilde{\Sigma}_{a(n)}^{11'} - \tilde{\Sigma}_{a(n)}^{22'}}{2}. \quad (32)$$

It is of notice that $\tilde{\Sigma}_{\text{odd}}$ is invariant under the rotation (20), the same being true for $\tilde{Z}_{a(n)}$, $\tilde{\Delta}_{a(n)}$, and $\tilde{E}_{a(n)}$, while this does not apply to $\tilde{\Sigma}_{a(n)}^{\text{even}'}$.

The results obtained from the solution of the Nambu-Gor'kov equation are collected in Table I, together with those of HFB and BCS. The fragments carrying the largest

fraction of the quasiparticle strength associated with each of the five valence orbitals of unperturbed energy ϵ_a are listed in order of increasing energy. For each fragment, the value of the renormalized quasiparticle energy $\tilde{E}_{a(n)}$, the renormalized quasiparticle amplitudes $\tilde{u}_{a(n)}$, $\tilde{v}_{a(n)}$, the renormalized single-particle energy $\tilde{\epsilon}_{a(n)}$, and the renormalized pairing gap $\tilde{\Delta}_{a(n)}$ are provided.

The formalism outlined above has been used to compute the two-nucleon transfer spectroscopic amplitudes

$$\begin{aligned} \tilde{B}[a(n)] &= \sqrt{\frac{2j_a + 1}{2}} \tilde{u}_{a(n)} \tilde{v}_{a(n)} \\ &= \sqrt{\frac{2j_a + 1}{2}} \int_{\tilde{E}_{a(n)} - \tilde{\Gamma}_{a(n)}/2}^{\tilde{E}_{a(n)} + \tilde{\Gamma}_{a(n)}/2} \tilde{S}^a(\omega) d\omega, \quad (33) \end{aligned}$$

associated with the reaction ${}^{120}\text{Sn}(p,t){}^{118}\text{Sn}(\text{g.s.})$ between two members of the Sn ground-state pairing rotational band, $\tilde{S}^a(\omega)$ being the anomalous component of the strength function associated with the dressed quasiparticle of energy $\tilde{E}_{a(n)}$ [Eq. (18)], expressed in the reduced space of the valence orbitals of the canonical basis. The corresponding results are shown in Table II, in comparison to those corresponding to the HFB and BCS calculation. Making use of global optical potentials (Table III), the absolute differential cross sections were calculated and are compared with the experimental findings in Fig. 4. Theory reproduces the experimental findings essentially at the 10% level (BCS 9.1%, HFB 13%, NFT (NG) 7%), well within experimental errors (see also Fig. 5). The stability of the theoretical results is apparent.

VII. DISCUSSION

The spectroscopic results reported in Table I testify to the important effects renormalization of the single-particle states and of the pairing interaction have at the level of quasiparticles. In spite of this, all three approaches [NFT (NG), HFB, BCS], notwithstanding their large differences in terms of many-body facets, predict essentially equally correct absolute two-nucleon-transfer cross sections, as testified by the results displayed in Figs. 4 and 5, where theory is compared to experiment.

It seems then fair to conclude that the quantity which controls the specific excitation of pairing rotational bands,

namely the order parameter α_0 , in the sense of Cooper pair transfer amplitude (Sec. III), is essentially invariant, whether calculated within the framework of the simplest one-pole quasiparticle (BCS) approximation or calculated by taking into account the variety of many-body renormalization effects.

The emergence of a physical sum rule is apparent (within this context, see Ref. [44], while for exact sum rules, see Refs. [45,46]). Let us elaborate on this point. By approximating

$$\tilde{u}_{a(n)} = \sqrt{N_{a(n)}}U_a, \quad \tilde{v}_{a(n)} = \sqrt{N_{a(n)}}V_a, \quad (34)$$

and

$$N_{a(n)} \approx Z_{a(n)} \approx Z_\omega \quad (\epsilon_a \approx \epsilon_F), \quad (35)$$

one can write

$$\alpha_0 = \sum_{a,n} \frac{2j_a + 1}{2} \tilde{u}_{a(n)} \tilde{v}_{a(n)} = \frac{N(0)}{Z_\omega} \int d\epsilon \frac{2j_\epsilon + 1}{2} \tilde{u}_\epsilon \tilde{v}_\epsilon, \quad (36)$$

where $N(0)/Z_\omega$ is the effective density of levels at the Fermi energy [21]. With the help of Eq. (35), one obtains

$$\alpha_0 = \frac{N(0)}{Z_\omega} Z_\omega \int d\epsilon \frac{2j_\epsilon + 1}{2} U_\epsilon V_\epsilon \approx \sum_a \frac{2j_a + 1}{2} U_a V_a. \quad (37)$$

The above relations are of no consequence, as they are trivially fulfilled, in the case in which the one-pole approximation to the quasiparticle level is valid, but they become relevant for those levels, like, e.g., the $d_{5/2}$ valence orbital, which undergo substantial fragmentation. Using each term of the expressions (36) and (37) as weighting factors of the corresponding two-nucleon-transfer form factors, in keeping with the unified structure-reaction physical interpretation of α_0 (Sec. III), and the result that (see Figs. 4 and 5) $|\sigma_i - \sigma_{\text{exp}}|/\sigma_{\text{exp}}$ is equal to 0.09, 0.13, and 0.07 ($i = \text{BCS, HFB, NG}$), the relative errors of the associated two-nucleon-transfer amplitudes $\alpha_0 (\sim \sqrt{\sigma})$ are 4.5%, 6.5%, and 3.5%.

Because the matrix elements of v_{14} for configurations based on the valence orbitals are essentially state independent and $Z^2 \approx 0.5$, setting $v_{\text{ind}} = 0$ one expects for the renormalized [NFT (NG)] cross section a value $\approx 1000 \mu b$ ($0.5 \times \sigma_{\text{HFB}}$), precluding the above accuracy. Consequently, on the basis of the validity of (36) and (37) and thus of the conservation of two-nucleon-transfer amplitudes in going from BCS mean field to NFT (NG) many-body, medium renormalization representations, one also finds the central role played by the induced pairing interaction.

ACKNOWLEDGMENTS

F.B. and E.V. acknowledge funding from the European Union Horizon 2020 research and innovation program, under Grant Agreement No. 654002. F.B. acknowledges funding from the Spanish Ministerio de Economía under Grant Agreement No. FIS2014-53448-C2-1-P. A.I. is supported by the Royal Society and Newton Fund through the Newton International Fellowship scheme.

APPENDIX A: OFF-DIAGONAL LONG-RANGE ORDER (ODLRO)

The challenge solved by Schrieffer [47] in his contribution to BCS was that of writing, starting from Cooper single-pair solution to pairing [48], a many-particle wave function in which each electron moving close to the Fermi energy participated in the condensate. The main problem is that N -fixed many-body wave functions cannot have a definite phase. But if one uses a coherent state representation, it is possible to describe a condensate with a definite phase. Schrieffer found a way to write down a coherent state of fermion pairs, namely (notice that primed quantities are again being used; see footnote 1),

$$|\text{BCS}\rangle = \Pi_{\nu>0} (U_\nu + V_\nu a_\nu^+ a_{\bar{\nu}}^+) |0\rangle. \quad (A1)$$

Introducing the phasing [18]

$$U_\nu = |U_\nu| = U'_\nu, \quad V_\nu = e^{-2i\phi} V'_\nu (V'_\nu \equiv |V_\nu|), \quad (A2)$$

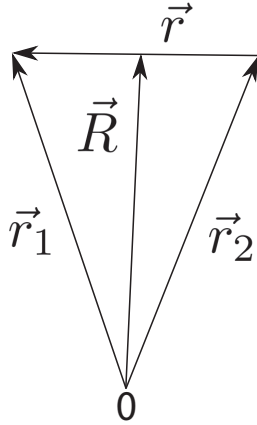
one can write

$$\begin{aligned} |\text{BCS}(\phi)\rangle_{\mathcal{K}} &= \Pi_{\nu>0} (U'_\nu + V'_\nu e^{-2i\phi} a_\nu^+ a_{\bar{\nu}}^+) |0\rangle \\ &= \Pi_{\nu>0} (U'_\nu + V'_\nu a_\nu^+ a_{\bar{\nu}}^+) |0\rangle = |\text{BCS}(0)\rangle_{\mathcal{K}'}, \end{aligned} \quad (A3)$$

where \mathcal{K} and \mathcal{K}' label the laboratory and the intrinsic (body-fixed BCS, deformed state in gauge space) frame of reference, while $a_\nu^+ = \mathcal{G}(\phi) a_\nu^+ \mathcal{G}^{-1}(\phi) = e^{-i\phi} a_\nu^+ (a_{\bar{\nu}}^+ = e^{-i\phi} a_{\bar{\nu}}^+)$ is a creation operator referred to this intrinsic frame. The operator $\mathcal{G}(\phi) = (\exp(-i\hat{N}\phi))$ induces a rotation of angle ϕ in gauge (two-dimensional) space (gauge transformation), where \hat{N} is the number of particle operator. The states $|\nu\rangle$ and $|\bar{\nu}\rangle$, connected by the time-reversal operator, have the same energy (Kramers' degeneracy).

A property of the above wave function, which has been given the name ‘‘off-diagonal long-range order’’ (ODLRO) [49], is of crucial importance regarding the physics at the basis of BCS condensation.¹¹ This property can be extracted

¹¹Within this context, let us quote from Ref. [50]: ‘‘It has become fashionable ... to assert ... that once gauge symmetry is broken, the properties of superconductors follow ...with no need to inquire into the mechanism by which the symmetry is broken. This is not ... true, since broken gauge symmetry might lead to molecule-like pairs and a Bose-Einstein [BEC, Feshbach resonance *our comment, see below*] rather than BCS condensation ... in 1957, we were aware that what is now called broken gauge symmetry would, under some circumstances (an energy gap or an order parameter), lead to many of the qualitative features of superconductivity. ...The major problem was to show how an energy gap, an order parameter of ‘condensation in momentum space’ could come about ...to show ...how the gauge-invariant symmetry of the Lagrangian could be spontaneously broken due to the interactions which were themselves gauge invariant’’ (p. 18). A Feshbach resonance is an enhancement in the scattering amplitude of a particle incident on a target—for instance, a nucleon scattering from a nucleus or an atom scattering from another one—when it has approximately the energy needed to create a quasibound state of the two-particle system. By making it feasible to precisely (Zeeman-tuned) control interactions, Feshbach resonances provide a tool for creating ultracold molecules and BECs.


 FIG. 6. Coordinates used to define the pair operator $P^+(\vec{R})$.

from the BCS wave function in a number of ways (see, e.g., Ref. [51])

To introduce the subject, let us start by writing down operators which create or annihilate pairs of fermions in the \vec{r} representation, i.e., by making use of $\psi^+(\vec{r}) = \langle \vec{r} | a_v^+ | 0 \rangle$ and the Hermitian conjugate. One can define the pair operator (see Fig. 6)

$$P^+(\vec{R}) = \int d^3r \phi(\vec{r}) \psi_v^+(\vec{R} + \vec{r}/2) \psi_v^+(\vec{R} - \vec{r}/2), \quad (\text{A4})$$

where $\phi(\vec{r})$ is the pair wave function. Thus $P^+(\vec{R})$ creates a spin singlet fermion pair where the particles are separated by the relative distance \vec{r} and with center of mass \vec{R} , i.e.,

$$\vec{R} = \frac{\vec{r}_1 + \vec{r}_2}{2}, \quad \vec{r} = \vec{r}_1 - \vec{r}_2, \quad (\text{A5})$$

and thus

$$\vec{r}_1 = \vec{R} + \frac{\vec{r}}{2}, \quad \vec{r}_2 = \vec{R} - \frac{\vec{r}}{2}. \quad (\text{A6})$$

One can now define a density matrix

$$\rho(\vec{R} - \vec{R}') = \langle P^+(\vec{R}) P(\vec{R}') \rangle, \quad (\text{A7})$$

that is, a generalized particle density for pairs, the so-called abnormal density, related to the two-particle density

$$\rho_2(\vec{r}_1\sigma_1, \vec{r}_2\sigma_2, \vec{r}_3\sigma_3, \vec{r}_4\sigma_4) = \langle \psi_v^+(\vec{r}_1) \psi_v^+(\vec{r}_2) \psi_v(\vec{r}_3) \psi_v(\vec{r}_4) \rangle. \quad (\text{A8})$$

Making use of the relations (A6) and (A7), one can write

$$\begin{aligned} \rho(\vec{R} - \vec{R}') &= \int d^3r d^3r' \phi(\vec{r}) \phi(\vec{r}') \\ &\times \rho_2(\vec{R} + \vec{r}/2, \sigma; \vec{R} - \vec{r}/2, -\sigma; \vec{R}' + \vec{r}'/2, \sigma; \\ &-\sigma; \vec{R}' - \vec{r}'/2, \sigma'). \end{aligned} \quad (\text{A9})$$

The pair wave function $\phi(\vec{r})$ vanishes when the relative distance becomes larger than the correlation length ξ . Thus, ρ is different from zero provided that $r(\equiv |\vec{r}_1 - \vec{r}_2|)$ and $r'(\equiv |\vec{r}_1' - \vec{r}_2'|)$ are smaller than ξ . But the pairs can be separated by any arbitrary distance. In other words, $\lim_{|\vec{R} - \vec{R}'| \rightarrow \infty} \rho(\vec{R} - \vec{R}') \neq 0$, that is, ODLRO. And this is what the |BCS> state ensures, in keeping with the fact that it describes independent

pair motion in which all pairs are in the same state, i.e.,

$$\begin{aligned} |\text{BCS}(\phi)\rangle_{\mathcal{K}} &= (\prod_{v>0} U'_v) \left\{ 1 + \sum_{v>0} c'_v e^{-2i\phi} a_v^+ a_v^+ \right. \\ &+ \frac{1}{2!} \left(\sum_{v>0} c'_v e^{-2i\phi} a_v^+ a_v^+ \right)^2 \\ &+ \frac{1}{3!} \left(\sum_{v>0} c'_v e^{-2i\phi} a_v^+ a_v^+ \right)^3 + \dots \left. \right\} \end{aligned} \quad (\text{A10})$$

where

$$c'_v = \frac{V'_v}{U'_v}. \quad (\text{A11})$$

This is the mean field solution of the pairing Hamiltonian. In other words, the ground state of the mean field pairing Hamiltonian

$$H_{MF} = U + H_{11}, \quad (\text{A12})$$

where

$$U = 2 \sum_{v>0} (\epsilon_v - \lambda) V_v^2 - \frac{\Delta^2}{G} \quad (\text{A13})$$

and

$$H_{11} = \sum_v E_v \alpha_v^+ \alpha_v. \quad (\text{A14})$$

Gauge symmetry restoration is obtained by taking into account the interaction

$$H''_p = \frac{G}{4} \left(\sum_{v>0} (\Gamma_v^+ - \Gamma_v) \right)^2, \quad (\text{A15})$$

acting among the quasiparticles, where $\Gamma_v^+ = \alpha_v^+ \alpha_v^+$. In fact, it can be shown that

$$[H_{MF} + H''_p, \hat{N}] = 0, \quad (\text{A16})$$

with \hat{N} being the number of particle operator. By diagonalizing Eq. (A15) in QRPA, i.e.,

$$[H_{MF} + H''_p, \Gamma_n^{''+}] = W_n'' \Gamma_n^+, \quad (\text{A17})$$

where

$$\Gamma_n^{''+} = \sum_{v>0} (a_{nv} \Gamma_v^+ + b_{nv} \Gamma_v), \quad (\text{A18})$$

the associated dispersion relation reads

$$\sum_{v>0} \frac{2E_v}{(2E_v)^2 - (W_n'')^2} = \frac{1}{G}, \quad (\text{A19})$$

while

$$a_{nv} = \frac{\Lambda_n''}{2E_v - W_n''}, \quad b_{nv} = \frac{\Lambda_n''}{2E_v + W_n''}, \quad (\text{A20})$$

with

$$\Lambda_n'' = \frac{1}{2} \left(\sum_{v>0} \frac{2E_v W_n''}{((2E_v)^2 - (W_n'')^2)} \right)^{-1/2}. \quad (\text{A21})$$

The lowest (most “collective”) root of Eq. (A19) has $W_1'' = 0$ (BCS gap equation), the associated eigenstate being

$$|1''\rangle = \Gamma_1''^+ |0\rangle = \Lambda_1'' \sum_{\nu>0} \frac{1}{2E_\nu} (\Gamma_\nu^+ + \Gamma_\nu) |0''\rangle. \quad (\text{A22})$$

In keeping with the fact that, in QRPA, the number operator reads

$$\tilde{N} = \Delta \sum_{\nu>0} \frac{1}{E_\nu} (\Gamma_\nu^+ + \Gamma_\nu) + N_0, \quad (\text{A23})$$

one can write

$$|1''\rangle = \Gamma_1''^+ |0''\rangle = \frac{\Lambda_1''}{2\Delta} (\tilde{N} - N_0) |0''\rangle. \quad (\text{A24})$$

A finite rotation in gauge space can be generated by a series of infinitesimal operations induced by the operator $\mathcal{G}(\phi) = \exp(-i\hat{N}\phi)$, i.e.,

$$\mathcal{G}(\delta\phi) \approx 1 - i\hat{N}\delta\phi. \quad (\text{A25})$$

Within this context, $i\{\mathcal{G}(\delta\phi) - [\mathcal{G}(0) - iN_0\delta\phi]\} = (\hat{N} - N_0)\delta\phi$, where $\delta\phi = \Lambda_1''/(2\Delta)$ [Eq. (A24)]. Because Λ_1'' diverges as $W_1'' \rightarrow 0$, $(\hat{N} - N_0)|\tilde{0}''\rangle \approx (\tilde{N} - N_0)|\tilde{0}''\rangle \rightarrow 0$, in keeping with Eq. (A16).

Divergence in gauge angle implies that ϕ can have any value in the range $0-2\pi$. Consequently, the system will be in a given member of a pairing rotational band, e.g.,

$$|N\rangle \sim \int d\phi e^{iN\phi} |\text{BCS}(\phi)\rangle_K \sim O^{N/2} |0\rangle, \quad (\text{A26})$$

where

$$O = \sum_{\nu>0} c'_\nu a_\nu^+ a_\nu^+. \quad (\text{A27})$$

One now rewrites O as

$$O = \int d^3r_1 d^3r_2 \chi(r_1, r_2) \psi_\uparrow^+(\vec{r}_1) \psi_\downarrow^+(\vec{r}_2) = \sum_k \chi(\vec{k}) a_{\vec{k}\uparrow}^+ a_{\vec{k}\downarrow}^+, \quad (\text{A28})$$

where $\chi(\vec{k}) = V'_k/U'_k$, and defines the normalized N -particle state as

$$|N\rangle = \mathcal{N}_N O^{N/2} |0\rangle \quad (\text{A29})$$

and the one-particle density matrix according to

$$\begin{aligned} \phi(\vec{r}_1, \vec{r}_1') &\equiv \langle N | \psi_\uparrow^+(\vec{r}_1) \psi_\uparrow(\vec{r}_1') | N \rangle \\ &= \langle N | \psi_\downarrow^+(\vec{r}_1) \psi_\downarrow(\vec{r}_1') | N \rangle. \end{aligned} \quad (\text{A30})$$

Making use of $\psi|0\rangle = 0$ and of the commutator

$$[\psi_\uparrow(\vec{r}_1), O^{N/2}] = \frac{N}{2} \int d^3r_2 \chi(\vec{r}_1, \vec{r}_2) \psi_\downarrow^+(\vec{r}_2) O^{(N-2)/2}, \quad (\text{A31})$$

one can write

$$\phi(\vec{r}_1, \vec{r}_1') = \int d^3r_2 \tilde{\chi}(\vec{r}_1', \vec{r}_2) \langle N | \psi_\uparrow^+(\vec{r}_1) \psi_\downarrow^+(\vec{r}_2) | N - 2 \rangle, \quad (\text{A32})$$

where

$$\tilde{\chi}(\vec{r}_1, \vec{r}_2) = (N/2) \mathcal{N}_N \mathcal{N}_{N-2}^{-1} \chi(\vec{r}_1, \vec{r}_2). \quad (\text{A33})$$

The matrix element in Eq. (A32) is closely related with Gorkov's amplitude for two fermions at \vec{r}_1 and \vec{r}_2 to belong to a Cooper pair, i.e.,

$$F^>(\vec{r}_1, \vec{r}_2) = -i \langle N - 2 | \psi_\uparrow(\vec{r}_1) \psi_\downarrow(\vec{r}_2) | N \rangle, \quad (\text{A34})$$

its complex conjugate being

$$\begin{aligned} F^>(\vec{r}_1, \vec{r}_2)^* &= i \langle N | \psi_\downarrow^+(\vec{r}_2) \psi_\uparrow^+(\vec{r}_1) | N - 2 \rangle \\ &= -i \langle N | \psi_\uparrow^+(\vec{r}_1) \psi_\downarrow^+(\vec{r}_2) | N - 2 \rangle. \end{aligned} \quad (\text{A35})$$

Thus, Eq. (A32) can be written as

$$\phi(\vec{r}_1, \vec{r}_1') = i \int d^3r_2 \tilde{\chi}(\vec{r}_1', \vec{r}_2) F^>(\vec{r}_1, \vec{r}_2)^*. \quad (\text{A36})$$

Let us now consider the two-particle matrix density

$$\begin{aligned} \phi(\vec{r}_1, \vec{r}_2; \vec{r}_3, \vec{r}_4) &\equiv \langle N | \psi_\uparrow^+(\vec{r}_1) \psi_\downarrow^+(\vec{r}_2) \psi_\downarrow(\vec{r}_4) \psi_\uparrow(\vec{r}_3) | N \rangle \\ &= \phi(\vec{r}_1, \vec{r}_3) \phi(\vec{r}_2, \vec{r}_4) + F^>(\vec{r}_1, \vec{r}_2)^* F^>(\vec{r}_3, \vec{r}_4), \end{aligned} \quad (\text{A37})$$

equivalent to

$$\begin{aligned} &\langle N | \psi_\uparrow^+(\vec{r}_1) \psi_\downarrow^+(\vec{r}_2) \psi_\downarrow(\vec{r}_4) \psi_\uparrow(\vec{r}_3) | N \rangle \\ &= \langle N | \psi_\uparrow^+(\vec{r}_1) \psi_\uparrow(\vec{r}_3) | N \rangle \langle N | \psi_\downarrow^+(\vec{r}_2) \psi_\downarrow(\vec{r}_4) | N \rangle \\ &\quad + \langle N | \psi_\uparrow^+(\vec{r}_1) \psi_\downarrow^+(\vec{r}_2) | N - 2 \rangle \langle N - 2 | \psi_\downarrow(\vec{r}_3) \psi_\uparrow(\vec{r}_4) | N \rangle. \end{aligned} \quad (\text{A38})$$

The function (A37) thus leads to a two-particle density matrix fulfilling

$$\begin{aligned} &\lim_{\vec{r}_1, \vec{r}_2 \rightarrow \infty; \vec{r}_3, \vec{r}_4 \rightarrow -\infty} \phi(\vec{r}_1, \vec{r}_2; \vec{r}_3, \vec{r}_4) \\ &= \lim_{\vec{r}_1, \vec{r}_2 \rightarrow \infty} [F^>(\vec{r}_1, \vec{r}_2)^*] \times [\lim_{\vec{r}_3, \vec{r}_4 \rightarrow -\infty} F^>(\vec{r}_3, \vec{r}_4)] \\ &\neq 0, \quad (r_{12}, r_{34} < \xi), \end{aligned} \quad (\text{A39})$$

a property known as ODLRO.

Within the nuclear embodiment, the wave function (A29) describes a member of a pairing rotation band, for example, the ground state of one of the superfluid Sn isotopes, in particular $^{120}\text{Sn}(\text{gs})$. In a reaction like $^{120}\text{Sn} + ^{118}\text{Sn} \rightarrow ^{118}\text{Sn}(\text{gs}) + ^{120}\text{Sn}(\text{gs})$, at energies where the distance of closest approach is $2R_o + a \approx 13$ fm ($E_{CM} \approx 270$ MeV), a number of the effects discussed above can materialize (Fig. 7). In the tunneling of a Cooper pair from a superfluid nucleus to the other, each partner can be in a different nucleus but still correlated. This is in keeping with the fact that the correlation length arising from the empirical pairing gap ($\Delta \approx 1.4$ MeV), resulting from the summed contribution of the bare and induced pairing interaction, is $\xi = \hbar v_F / \pi \Delta \approx 12$ fm.

Let us go back to the QRPA (harmonic) diagonalization of $H = H_{MF} + H_p''$. One can rewrite H as the oscillator [2],

$$H = \frac{p^2}{2D_1''} + \frac{1}{2} D_1'' \omega_1'' q^2, \quad (\text{A40})$$

and identify the momentum with the number operator, the coordinate with the gauge angle, and the frequency with the QRPA energy,

$$p = \hbar(\tilde{N} - N_0), \quad q = \phi, \quad \hbar\omega_1'' = W_1''. \quad (\text{A41})$$

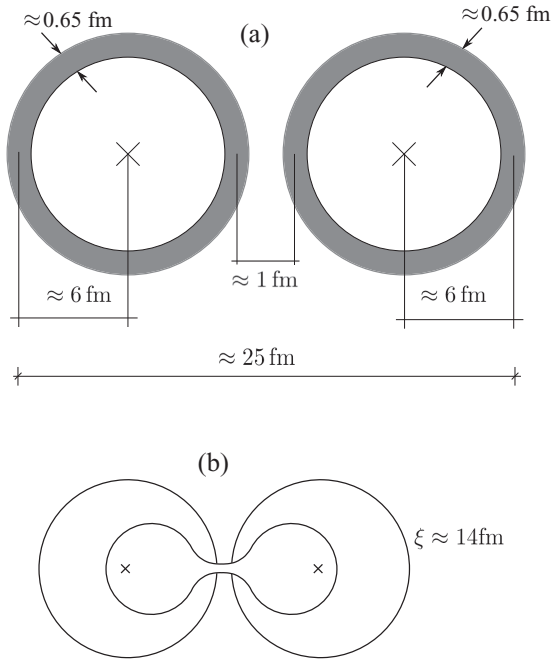


FIG. 7. (a) Schematic representation of two Sn nuclei at a distance of closest approach of ≈ 13 fm. (b) Single Cooper pair in which each nucleon is in a different nucleus.

The phonon creation operator for the oscillator is

$$\Gamma_1^{\prime\prime+} = \sqrt{\frac{\hbar^2}{2D_1''W_1''}}(\tilde{N} - N_0) + i\phi\sqrt{\frac{D_1''W_1''}{2\hbar^2}}. \quad (\text{A42})$$

Comparing the coefficient of $(\tilde{N} - N_0)$ in Eqs. (A24) and (A42), and noting that the coefficient of ϕ in Eq. (A42) vanishes in the limit $W_1'' \rightarrow 0$, we get an expression for the mass parameter

$$\frac{\hbar^2}{2D_1''W_1''} = \left(\frac{\Lambda_1''}{2\Delta}\right)^2 \quad (\text{A43})$$

or

$$\frac{D_1''}{\hbar^2} = \frac{4\Delta^2}{2W_1''\Lambda_1''^2}. \quad (\text{A44})$$

Making use of Eq. (A21), one obtains

$$\frac{1}{W_1''\Lambda_1''^2} = 4 \sum_{\nu>0} \frac{2E_\nu}{[(2E_\nu)^2 - (W_1'')^2]^2}. \quad (\text{A45})$$

In the limit $W_1'' \rightarrow 0$, this relation becomes

$$\frac{1}{W_1''\Lambda_1''^2} = \sum_{\nu>0} \frac{1}{2E_\nu^3}, \quad (\text{A46})$$

and the mass parameter can be written as

$$\frac{D_1''}{\hbar^2} = \sum_{\nu>0} \frac{\Delta^2}{E_\nu^3}, \quad (\text{A47})$$

an emergent property of generalized rigidity in gauge space for a nucleus whose mean field solution violates gauge invariance.

By making use of Eq. (A47) and of the fact that $\lambda = \partial H / \partial N$, the energy of the members of a pairing rotational band can be written as

$$E_N = \lambda N + \frac{\hbar^2}{2\mathcal{J}}N^2, \quad (\text{A48})$$

where

$$\frac{\mathcal{J}}{\hbar^2} = \frac{D_1''}{\hbar^2} = \sum_{\nu>0} \frac{4U_\nu'^2 V_\nu'^2}{E_\nu} = 2 \sum_{\nu>0} \frac{\langle \nu \bar{\nu} | \hat{N} | \text{BCS} \rangle^2}{2E_\nu} \quad (\text{A49})$$

is the cranking formula of the moment of inertia of rotation in gauge space. Pairing rotations can be viewed as the Goldstone mode, or better the Anderson-Goldstone-Nambu mode [3,4,6–8] in gauge space, approaching the $E = 0$ limit linearly with N . This is in keeping with the fact that such behavior is only expected in the laboratory system, where it can be measured. In other words, by summing to the BCS energy U [Eq. (A13)], the Coriolis force in gauge space λN felt by the condensate in the intrinsic system.

APPENDIX B: NFT VACUUM POLARIZATION

The role zero-point fluctuations play in the nuclear ground state, i.e., in the NFT vacuum, can be clarified by relating it to the polarization of the QED vacuum. Let us briefly dwell on the “reality” of such phenomenon by recalling the fact that Lamb gave a quantitative answer, both experimentally and theoretically [52,53], to Rabi’s question of whether the polarization of the QED vacuum could be measured [54], in particular, the change in charge density felt by the electrons of an atom, e.g., the electron of a hydrogen atom, due to virtual creation and annihilation of electron-positron pairs. The corresponding correction (Lamb shift) implies that the $^2S_{1/2}$ level lies higher than the $^2P_{1/2}$ level by about 1000 MHz, as experimentally observed.

In connection with the discussion of vacuum polarization, where a field produces a pair and the subsequent pair annihilation produces a new field, namely a closed loop, Feynman implemented in his space-time trajectories Wheeler’s idea of electrons going backward in time (positrons). Such trajectories would be like an \mathbf{N} in time, that is, electrons which would back up for a while and then go forward again. Being connected with a minus sign, these processes are associated with Pauli principle in the self-energy of electrons [see Fig. 1(I)(c)]. The divergences affecting such calculations could be renormalized by first computing the self-energy diagram in second order and finding the answer, which is finite but contains a cutoff to avoid a logarithmic divergence. Expressing the result in terms of the experimental mass, one can take the limit (cutoff $\rightarrow \infty$) which now exists. Concerning radiative corrections to scattering, in particular that associated with the process in which the potential creates an electron-positron pair which then reannihilates, emitting a quantum which scatters the electron, the renormalization procedure should be applied to the electric charge, introducing the observed one (Bethe and Pauli; see Ref. [55]).

In the nuclear case, for example, Skyrme effective interactions give rise to particle-vibration coupling vertices which, because of the contact character of these interactions,

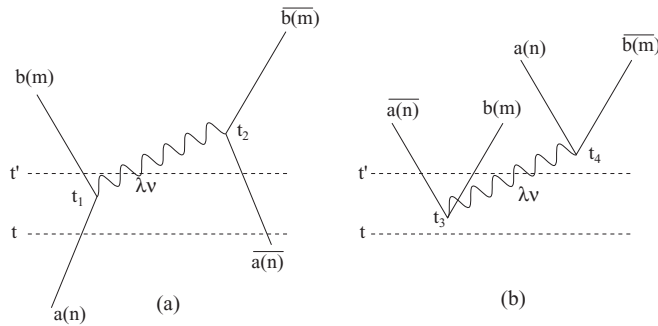


FIG. 8. Schematic representation of the induced pairing interaction (29).

may lead to divergent zero-point energies, unless a cutoff is introduced.¹² The Gogny force, being finite range, does not display such problems. Nonetheless, the associated results concerning zero-point energies may not be very stable and/or accurate when carrying out a complete summation over both collective and noncollective contributions. In this case, one can eliminate such a problem by going to higher orders in the oyster diagrams [see Fig. 1(I)(a)]. The fermion exchange between two of these diagrams (Pauli principle) essentially eliminates all of the noncollective contributions.

An economic and quite reliable method to achieve a similar result is that of using NFT renormalization, that is, calculating the lowest order diagrams but introducing, in the intermediate states, the dressed physical (empirical) states ([33,56]; see also Ref. [57]).

APPENDIX C: STATE-DEPENDENT EFFECTIVE MASS AND MEAN FIELD POTENTIAL

The bare mass of a nucleon in the nucleus is not a quantity that can be measured. This is because a nucleon in the nucleus is subject to a mean field which is nonlocal in both space and time.

The first component arises at the level of Hartree-Fock and is directly related to the Hartree exchange potential, assuming velocity-independent interactions. This nonlocality can be taken care of, in most situations, in terms of an effective mass, the k mass, with its average value being $m_k \approx 0.7m$, where m is the observed nucleon mass. The quantity m_k is intimately related to the so-called Perey-Buck potential, namely the energy-dependent term in the strength $V = V_0 + 0.4E$ of the

¹²The velocity-dependent component of these forces also weakens the PVC vertices, leading to poorly collective low-lying vibrations and to equally poorly clothed valence states. The question then emerges, about which are the provisos to be taken in the use of effective forces to higher orders of the PVC, concerning the implementation of renormalization in both configuration and 3D spaces within the framework of NFT (see Refs. [30,32,33])? In a nutshell, the bare mean field exists but its properties cannot be measured (any more than the bare electron mass in renormalized quantum electrodynamics) and corresponds to a set of parameters of a Fermi-like function which ensure that the clothed states reproduce the experimental findings, both structural and reaction.

real part of the optical potential needed to describe nucleon-nucleus elastic scattering experiments at bombarding energies of tens of MeV, where $E = |\epsilon_k - \epsilon_F|(\epsilon_k = \hbar^2 k^2 / 2m)$. One can obtain essentially the same results by solving the elastic scattering single-particle Schrödinger equation, making use of an energy-independent potential of strength $V \approx (m/m_k)V_0 = 1.4V_0$ and an effective mass $m_k = [1 + (m/\hbar^2 k)dV/dk]^{-1}$ (within this context, see Fig. 2.14 of Ref. [22]). Similar results and protocol are obtained and can be used to describe deep hole states.

In other words, the concept of a single, mean field potential is a somewhat illusory one. This is in keeping with the fact that there is not a single m_k , but a state-dependent one equal to the expectation value of the quantity in parentheses, where V is now the sum of the direct and exchange potentials, calculated by making use of the corresponding single-particle wave functions [58].

Retardation effects arise from the coupling of single particles with collective vibrations [Fig. 1(I)]. They lead, for states close to the Fermi energy, to the state-dependent ω mass [$m_\omega = m(1 + \lambda)$, $Z_\omega = m/m_\omega$] and to fragmentation, effects which can hardly be parameterized in terms of an average mean field potential.

In other words, the above effects are at the basis of the dynamical shell model. While one can, within this context, accurately calculate the single-particle properties [$\tilde{\epsilon}_{a(n)}$, $\tilde{Z}_{a(n)}$, $\tilde{N}_{a(n)}$] in simple and economic ways, e.g., renormalized NFT, the situation is much more complex concerning the absolute value of the Fermi energy.

APPENDIX D: INDUCED PAIRING INTERACTION

The exchange of collective vibrations between nucleons moving in time-reversal states gives rise to an induced,

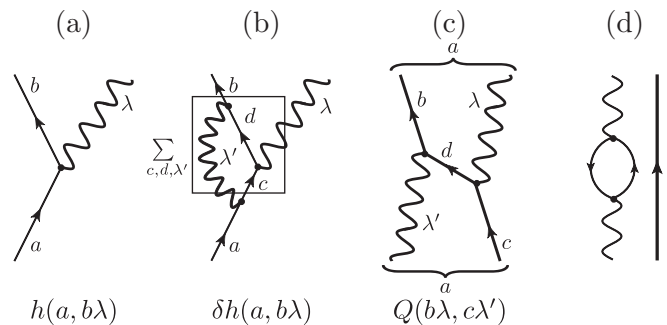


FIG. 9. Particle-vibration coupling (PVC) vertex renormalization of the induced pairing interaction. (a) PVC $h(a, b, \lambda)$. (b) Vertex renormalization $\delta h(a, b, \lambda)$. (c) This diagram summed over d [see Eqs. (E1) and (E2)] corresponds to one of those describing Compton scattering in quantum electrodynamics and resulting from the time ordering of the Pauli principle correction between the single nucleon considered explicitly and those out of which the vibrations are built, shown in panel (d). In fact, it can be obtained from such process by time ordering and corresponds to the symmetrization of the phonon renormalizing the fermion $|c\rangle$ (self-energy process) and an external phonon (see, e.g., [60]). It is of notice that the quantity $h(a, c\lambda'v')/[E_a - (E_c + \hbar\omega_{\lambda'v'})]$ in (E1) is the amplitude with which the state $|a\rangle$ is in the state $|c\lambda'\rangle$ [boxed process in diagram (b)].

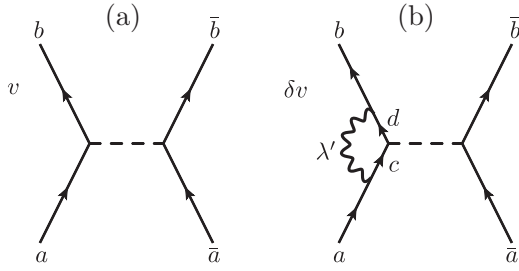


FIG. 10. Particle-vibration coupling (PVC) vertex renormalization of the bare pairing interaction. (a) Process through which two nucleons moving in time-reversal states interact through the bare pairing interaction. (b) Vertex renormalization through the PVC.

medium polarization, pairing interaction. In the quasiparticle representation and QRPA treatment of the collective modes, the different lowest order contributions in the PVC vertices to (29) are shown in Fig. 8 [see Figs. 1 II(e)–(g) for examples of higher order]. To each vertex is associated a function $h(a(n), b(m)\lambda\nu)$. The denominator corresponds to the energy difference between the configuration at time t and at time t' , i.e.,

$$\begin{aligned} \text{(a)} &= \sum_{\lambda\nu} \frac{2|h(a(n), b(m)\lambda\nu)|^2}{\tilde{E}_{a(n)} - \tilde{E}_{b(m)} - \hbar\omega_{\lambda\nu}} \quad \text{and} \\ \text{(b)} &= - \sum_{\lambda\nu} \frac{2|h(a(n), b(m)\lambda\nu)|^2}{\tilde{E}_{a(n)} + \tilde{E}_{b(m)} + \hbar\omega_{\lambda\nu}}, \end{aligned} \quad (\text{D1})$$

the factor of 2 arising from the two time-ordered contributions, i.e., $t_1 < t_2$ and $t_2 > t_1$, and $t_3 < t_4$ and $t_4 > t_3$ respectively. Lines without arrows represent quasipar-

ticles, the wavy line denotes QRPA vibrations of multipolarity λ , and increasing energy is labeled by ν .

APPENDIX E: VERTEX CORRECTIONS

The PVC mechanism gives rise to self-energy processes [e.g., Figs. 1(II)(a), 1(II)(c), and 1(II)(d)] but also to vertex renormalization [Fig. 1(II)(e)]. In other words, $h(a, b\lambda\nu)$ [Fig. 9(a)] is to be corrected to lowest order in the PVC vertex [Fig. 9(b)], a correction which can be written as

$$\delta h(a, b\lambda\nu) = \sum_{c, \lambda' \nu'} \frac{Q(b\lambda\nu, c\lambda'\nu')h(a, c\lambda'\nu')}{\tilde{E}_a - (E_c + \hbar\omega_{\lambda'\nu'})}, \quad (\text{E1})$$

where [Fig. 9(c)]

$$\begin{aligned} Q(b\lambda\nu, c\lambda'\nu') &= \sum_d h(b, d\lambda'\nu') \\ &\times \frac{\langle (j_d\lambda')j_b, \lambda; j_a | (j_d\lambda)j_c, \lambda'; j_a \rangle}{\tilde{E}_a - (E_d + \hbar\omega_{\lambda\nu} + \hbar\omega_{\lambda'\nu'})} h(c, d\lambda\nu), \end{aligned} \quad (\text{E2})$$

with $\langle (j_d\lambda')j_b, \lambda; j_a | (j_d\lambda)j_c, \lambda'; j_a \rangle$ being a recoupling coefficient.

Correction (E1), with the proper indexing, has to be added to both vertices entering the expression for v_{ind} , as well as to those of the various self-energies. In the case under discussion, namely, ^{120}Sn , that is, a medium-heavy superfluid nucleus lying along the stability valley, the recoupling coefficient [Eq. (E2)] displays random phases, leading to strong cancellations when summed over the different quantum numbers and resulting in values of δh of the order of few tens of keV.

Similar arguments apply to the bare pairing interaction vertex correction [Fig. 10(b)].

-
- [1] B. R. Mottelson, Elementary features of nuclear structure, in *Trends in Nuclear Physics. 100 Years Later*, Les Houches, Session LXVI (Elsevier, Amsterdam, 1998), p. 25.
- [2] D. M. Brink and R. A. Broglia, *Nuclear Superfluidity* (Cambridge University Press, Cambridge, UK, 2005).
- [3] A. Bohr and B. R. Mottelson, *Nuclear Structure* (Benjamin, New York, 1975), Vol. 2.
- [4] D. R. Bes and R. A. Broglia, Pairing vibrations, *Nucl. Phys.* **80**, 289 (1966).
- [5] R. A. Broglia, Nuclear structure then and now: 40 years of the 1975 Nobel Prize in physics, *Ann. Phys.* **528**, 444 (2016).
- [6] R. A. Broglia, J. Terasaki, and N. Giovanardi, The Anderson-Goldstone-Nambu mode in finite and infinite systems, *Phys. Rep.* **335**, 1 (2000).
- [7] N. Inohara and W. Nazarewicz, Nambu-Goldstone Modes with Nuclear Density Functional Theory, *Phys. Rev. Lett.* **116**, 152502 (2016).
- [8] N. L. Vaquero, J. L. Egido, and T. R. Rodríguez, Large-amplitude pairing fluctuations in atomic nuclei, *Phys. Rev. C* **88**, 064311 (2013).
- [9] W. Heisenberg, About the constitution of atomic nuclei, 1, *Zeit. Phys.* **77**, 1 (1932).
- [10] M. G. Mayer, Nuclear configurations in the spin-orbit coupling model, 2: Theoretical considerations, *Phys. Rev.* **78**, 22 (1950).
- [11] G. Racah and I. Talmi, The pairing properties of nuclear interactions, *Phys. (Amsterdam, Neth.)* **18**, 1097 (1952).
- [12] J. Bardeen, L. N. Cooper, and J. R. Schrieffer, Microscopic theory of superconductivity, *Phys. Rev.* **106**, 162 (1957).
- [13] J. Bardeen, L. N. Cooper, and J. R. Schrieffer, Theory of superconductivity, *Phys. Rev.* **108**, 1175 (1957).
- [14] A. Bohr, B. R. Mottelson, and D. Pines, Possible analogy between the excitation spectra of nuclei and those of the superconducting metallic state, *Phys. Rev.* **110**, 936 (1958).
- [15] A. Bohr, Elementary modes of excitation and their coupling, *Comptes Rendus du Congrès International de Physique Nucléaire*, Vol. I, edited by I. P. Gugenberg (Editions du Centre National de la Recherche Scientifique, Paris, 1964), p. 487.
- [16] S. Yoshida, Note on the two-nucleon stripping reaction, *Nucl. Pays.* **33**, 685 (1962).
- [17] G. Potel, A. Idini, F. Barranco, E. Vigezzi, and R. A. Broglia, Quantitative study of coherent pairing modes with two-neutron transfer: Sn isotopes, *Phys. Rev. C* **87**, 054321 (2013).

- [18] J. R. Schrieffer, Microscopic quantum phenomena from pairing in superconductors, *Phys. Today* **26**(7), 23 (1973).
- [19] G. Potel, A. Idini, F. Barranco, E. Vigezzi, and R. A. Broglia, Cooper pair transfer in nuclei, *Rep. Prog. Phys.* **76**, 106301 (2013).
- [20] S. Baroni, M. Armati, F. Barranco, R. A. Broglia, G. Colò, G. Gori, and E. Vigezzi, Correlation energy contribution to nuclear masses, *J. Phys. G* **30**, 1353 (2004).
- [21] F. Barranco, P. F. Bortignon, R. A. Broglia, G. Colò, P. Schuck, E. Vigezzi, and X. Viñas, Pairing matrix elements and pairing gaps with bare, effective, and induced interactions, *Phys. Rev. C* **72**, 054314 (2005).
- [22] C. Mahaux, P. F. Bortignon, R. A. Broglia, and C. H. Dasso, Dynamics of the shell model, *Phys. Rep.* **120**, 1 (1985).
- [23] W. H. Dickhoff and D. Van Neck, *Many-Body Theory Exposed! Propagator Description of Quantum Mechanics in Many-Body Systems* (World Scientific, Singapore, 2008).
- [24] M. Born, *Natural Philosophy of Cause and Chance* (Clarendon Press, Oxford, UK, 1949).
- [25] J. Schwinger, *Quantum Electrodynamics* (Dover, New York, 1958).
- [26] R. P. Feynman, *Quantum Electrodynamics* (Benjamin, New York, 1962).
- [27] J. Mehra, *The Beat of a Different Drum* (Oxford University Press, Oxford, 1994), p. 235.
- [28] R. A. Broglia, O. Hansen, and C. Riedel, Two-neutron transfer reactions and the pairing model, *Adv. Nucl. Phys.* **6**, 287 (1973), see <http://www.mi.infn.it/~vigezzi/BHR/BrogliaHansenRiedel.pdf>.
- [29] F. Barranco, R. A. Broglia, G. Colò, G. Gori, E. Vigezzi, and P. F. Bortignon, Many-body effects in nuclear structure, *Eur. J. Phys. A* **21**, 57 (2004).
- [30] A. Idini, G. Potel, F. Barranco, E. Vigezzi, and R. A. Broglia, Interweaving of elementary modes of excitation in superfluid nuclei through particle-vibration coupling: Quantitative account of the variety of nuclear structure observables, *Phys. Rev. C* **92**, 031304(R) (2015).
- [31] A. Bracco, P. F. Bortignon, and R. A. Broglia, *Giant Resonances* (Harwood, Amsterdam, 1998).
- [32] R. A. Broglia, P. F. Bortignon, F. Barranco, E. Vigezzi, A. Idini, and G. Potel, Unified description of structure and reactions: Implementing the nuclear field theory program, *Phys. Scr.* **91**, 063012 (2016).
- [33] F. Barranco, G. Potel, R. A. Broglia, and E. Vigezzi, Structure and Reactions of ^{11}Be : Many-Body Basis for Single-Neutron Halo, *Phys. Rev. Lett.* **119**, 082501 (2017).
- [34] L. P. Gor'kov, On the energy spectrum of superconductors, *Soviet Physics JETP-USSR* **7**, 505 (1958).
- [35] Y. Nambu, Quasiparticles and gauge invariance in the theory of superconductivity, *Phys. Rev.* **117**, 648 (1960).
- [36] G. M. Eliashberg, Interactions between electrons and lattice vibrations in a superconductor, *Soviet Physics JETP-USSR* **11**, 696 (1960).
- [37] D. R. Bes and R. A. Sorensen, The pairing-plus-quadrupole model, *Adv. Nucl. Phys.* **2**, 129 (1969).
- [38] A. Idini, Ph.D. thesis, University of Milano, Milan, Italy, 2012 (unpublished), http://dx.doi.org/10.13130/2Fidini-andrea_phd2013-02-05.
- [39] A. L. Fetter and J. D. Walecka, *Quantum Theory of Many-Particle Systems* (McGraw-Hill, New York, 1971).
- [40] A. Pastore, F. Barranco, R. A. Broglia, and E. Vigezzi, Microscopic calculation and local approximation of the spatial dependence of the pairing field with bare and induced interactions, *Phys. Rev. C* **78**, 024315 (2008).
- [41] J. Terasaki, F. Barranco, R. A. Broglia, E. Vigezzi, and P. F. Bortignon, Solution of the Dyson equation for nucleons in the superfluid phase, *Nucl. Phys. A* **697**, 127 (2002).
- [42] A. Idini, F. Barranco, and E. Vigezzi, Quasiparticle renormalization and pairing correlations in spherical superfluid nuclei, *Phys. Rev. C* **85**, 014331 (2012).
- [43] P. Guazzoni, L. Zetta, A. Covello, A. Gargano, B. F. Bayman, T. Faestermann, G. Graw, R. Hertenberger, H.-F. Wirth, and M. Jaskola, ^{118}Sn levels studied by the $^{120}\text{Sn}(p,t)$ reaction: High-resolution measurements, shell model, and distorted-wave Born approximation calculations, *Phys. Rev. C* **78**, 064608 (2008).
- [44] R. A. Broglia, C. Riedel, and T. Udagawa, Sum rule and two-particle units in the analysis of two-nucleon transfer reactions, *Nucl. Phys. A* **184**, 23 (1972).
- [45] B. F. Bayman and C. F. Clement, Sum Rules for Two-Nucleon Transfer Reactions, *Phys. Rev. Lett.* **29**, 1020 (1972).
- [46] W. A. Lanford, Systematics of two-neutron transfer cross sections near closed shells: A sum-rule analysis of (p,t) strength on the lead isotopes, *Phys. Rev. C* **16**, 988 (1977).
- [47] J. R. Schrieffer, *Superconductivity* (Benjamin, New York, 1964).
- [48] L. N. Cooper, Bound electron pairs in a degenerate Fermi gas, *Phys. Rev.* **104**, 1189 (1956).
- [49] C. N. Yang, Concept of off-diagonal long-range order and the quantum phase of liquid He and of superconductors, *Rev. Mod. Phys.* **34**, 694 (1962).
- [50] L. N. Cooper, Remembrance of superconductivity past, in *BCS: 50 Years*, edited by L. N. Cooper and D. Feldman (World Scientific, Singapore, 2010), p. 3.
- [51] V. Ambegaokar, The Green's function method, in *Superconductivity*, edited by R. D. Parks (Marcel Dekker, New York, 1969), Vol. 1, p. 259.
- [52] W. E. Lamb, Jr. and R. C. Retherford, Fine structure of the hydrogen atom by a microwave method, *Phys. Rev.* **72**, 241 (1947).
- [53] N. M. Kroll and W. E. Lamb, Jr., On the self-energy of a bound electron, *Phys. Rev.* **75**, 388 (1949).
- [54] A. Pais, *Inward Bound* (Oxford University Press, Oxford, UK, 1986).
- [55] R. P. Feynman, Space-time approach to quantum electrodynamics, *Phys. Rev.* **76**, 769 (1949).
- [56] R. D. Mattuck, *A Guide to Feynman Diagrams in the Many-Body Problem* (Dover, New York, 1976).
- [57] D. R. Bes, G. G. Dussel, R. P. J. Perazzo, and H. M. Sofia, The renormalization of single-particle states in nuclear field theory, *Nucl. Phys. A* **293**, 350 (1977).
- [58] V. Bernard and N. Van Giai, Single-particle and collective nuclear states and the Green's function method, in *Nuclear structure and heavy ion collisions, Proc. Int. School of Physics E. Fermi, Course LVII*, edited by R. A. Broglia, R. A. Ricci, and C. H. Dasso (North Holland, Amsterdam, 1981), p. 437.
- [59] H. An and C. Cai, Global deuteron optical model potential for the energy range up to 183 MeV, *Phys. Rev. C* **73**, 054605 (2006).
- [60] B. R. Mottelson, Elementary modes of excitation in the nucleus, *Rev. Mod. Phys.* **48**, 375 (1976).